A thesis submitted in fulfilment of the requirements for the degree of Master of Science (M.Sc.) in Applied Geoinformatics

Department of Environmental Remote Sensing & Geoinformatics

University of Trier

Evaluation of MODIS-derived phenological parameters using ground based observations

---

Author:

Hendrik Bernert

Matr.-No.: 1126611

✉ s6hebern@uni-trier.de

Supervisors:

Dr. Sebastian Mader & Dr. Marion Stellmes

submitted: September 9, 2015

Abstract

Plant phenology can be assessed from remotely sensed vegetation indices. A spline framework (*splits*) has been used to model a MODIS-derived EVI time series for Germany from 2001 to 2014. The program provides the user with a graphical interface to fit an appropriate function to the raw EVI time series and to extract phenological descriptors from it. The results have been compared to ground based observations from the German Weather Service (DWD). At best, the difference between the modelled and the reference dates for the start of the growing season was less than a week (depending on the respective plant species). The outcomes strongly depend on the crucial greenness parameter g, indicating the onset of greening as a percentage of the annual EVI amplitude. However, this value has shown to be species-dependent and much higher than described in the literature. Especially winter crops cause problems due to their shifted growing cycle, but forest stands can be modelled to show an overall good agreement with the reference data. From the spatial patterns of some of the extracted phenological descriptors, land use classes can be identified by comparing those maps to the CORINE Land Cover dataset. Since the phenological parameters can be characteristic for different plant species, future classification frameworks might make use of them to create not only land use, but also land cover classifications.

Contents

List of Figures

List of Tables

Abbreviations

CLC	CORINE Land Cover
DOY	day of the year
DWD	German Weather Service (Deutscher Wetterdienst)
EOG	end of greening
EVI	Enhanced Vegetation Index
GDD	growing degree days
MODIS	Moderate-Resolution Imaging Spectroradiometer
NDVI	Normalized Difference Vegetation Index
NIR	near-infrared
SOG	start of greening
VI	vegetation index

Acknowledgements

This thesis would not have been possible without the help of numerous people.

I gratefully acknowledge the support and prolific input from my supervisors, Dr. Sebastian Mader and Dr. Marion Stellmes, who not only gave me the opportunity to write a thesis about this interesting topic, but also gave me hints, advices and helpful ideas during the whole process.

David Frantz wrote the *modis-prepro*-tool to create time series from MODIS vegetation index products, which has been very helpful and saved me a lot of time.

Prof. Dr. Joachim Hill gave me the opportunity of working within the *SuMaRio* project as a student assistant, which broadened my skillset and gave me interesting insights into the topics of atmospheric correction and time series analysis.

Special thanks to Thomas Rommel, who not only supported me during countless hours of programming, but also for critical ideas, helpful discussions, revising this thesis and being a magnificent friend from the beginning.

I also want to thank Barbara Paschmionka, Laura Leimbrock, Erik Haß, Andreas Löwe and all of my other student colleagues for their friendship and help throughout my studies.

A very warm "Thank you" to Caitlin Derbeck for her love and patience, for welcome distractions and sustaining me from the beginning. Finally, to my family and friends, who always encouraged me, spent time discussing the topics of this thesis and gave me overall support whenever needed.

1

Introduction

Assessing plant phenology from spaceborn imagery has been a major interest for the scientific community for more than a decade. Phenological parameters like greenup, maturity or senescence are visible in vegetation index (VI) profiles, showing a plant's annual development (Zhang et al., 2001). Several studies have dealt with this subject, using different sensors and methods to model the course of one or another VI through time and extract parameters like the onset of greening or the length of the growing season. To achieve this, VI measurements have to be combined to a time series, which must be described mathematically. Afterwards, distinct points along the temporal profile of the VI can be identified and assigned to specific phenological events in a plant's annual development (see Figure 1.1).

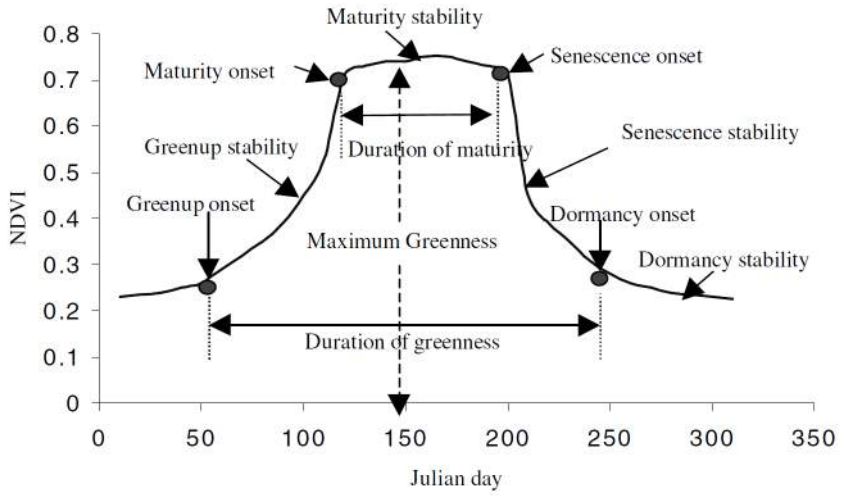

Figure 1.1: Phenological parameters can be identified in a NDVI profile (Zhang et al., 2001).

1.1 Vegetation indices

Vegetation indices take advantage of the differences in the absorption and reflection of light when it strikes a vegetated surface. For vital vegetation, this difference occurs in the red and near-infrared (NIR) ranges of the electromagnetic spectrum. For red, most of the light's energy is absorbed, while the contrary is true for NIR (Jackson and Huete, 1991). Using that difference in reflection, indices can be set up like the Normalized Difference Vegetation Index (NDVI), which is defined as

$$NDVI = \frac{NIR - red}{NIR + red}$$

and ranges between -1 and $+1$. It is widely used and can be derived very easily, without any further input variables. Another important VI is the Enhanced Vegetation Index (EVI), which includes corrections for disturbances in the reflected light caused by atmospheric particles (like aerosols) and the ground cover below the vegetation (Meier and Herring, 2000). It is calculated by

$$EVI = G * \frac{NIR - red}{NIR + C_1 * red - C_2 * blue + L}$$

with G, C_1, C_2 and L as the adjusting factors from the canopy background (L), aerosol influences (C_1 & C_2) and an additional scaling parameter (G) (Solano et al., 2010). Because of these correcting factors, it may be seen as the more exact VI compared to the NDVI, but the uncertainties and additional assumptions for the correction factors make it more vulnerable for errors.

These two indices are automatically calculated for each scene collected by the Moderate-Resolution Imaging Spectroradiometer (MODIS), a multispectral satellite system run by the United States Geological Survey. It covers the whole earth on a daily basis with a ground resolution of up to 250 m (depending on the final product). Other satellite systems, like *Landsat* for instance, have a better spatial resolution, but the user has to calculate the VI manually. For very simple ones, like

the NDVI, this should not cause any problems, but for the EVI, this might make results from different studies incomparable, if the correction factors are estimated differently. No matter how the final VI data are obtained, such images, having the same extent and spatial resolution, can be stacked together to make up a time series, with each band representing one time step. Afterwards, every pixel within this stacked image includes its own unique time series of VI data for that specific location.

1.2 Deriving phenological parameters

To derive phenological parameters from a VI profile as indicated by Zhang et al., the time series has to be described mathematically. Different approaches of modelling data like this have been developed, each of them with its own benefits and drawbacks. Once a suitable mathematical function (or a set of functions) is found that describes the time series best, it can be modelled and the phenological descriptors can be derived.

An early approach of using VI data for the extraction of phenological parameters was done by Zhang et al., who fitted piecewise logistic functions to a MODIS derived EVI time series of one year. The dates for the onset of the main phenological stages, measured in day of the year (DOY), were then extracted by analyzing the rate of change in the curvature of the fitted model. For their study site in North America, they state their results as "realistic", but had no validation data to verify their findings (Zhang et al., 2003).

Soudani et al. used MODIS NDVI data, to which they fitted an asymmetric double-sigmoid function to extract the onset of greenup in deciduous forest stands. They compared the results to ground based NDVI measurements at discrete locations across France over a period of five years (2000 - 2004). Using different points along the modelled curve, the best agreement between model predictions and in-situ measurements of the NDVI created a prediction uncertainty of 8.5 days, with a bias of 3.5 days (Soudani et al., 2008).

This approach has been used and improved by Hmimina et al., who studied different regions and also expanded the time series until 2009. Additionally, leaf senescence in autumn has been taken into account. For deciduous forests, they were able to decrease the prediction uncertainty to less than a week and also detected a strong influence of noise in the NDVI data, which distorts the time series and its mathematical representation. Especially in rainforest areas, this causes errors and shifts in the derived phenological dates (Hmimina et al., 2013).

Böttcher et al. extracted the onset of the growing season for pine stands in Finland from smoothed MODIS NDVI data. They used adaptive Savitzky–Golay filtering to reduce noise in the time series, from which the start of greening (SOG) was then determined as the last day between February 1^{st} and July 19^{th} with an NDVI value below the annual NDVI minimum plus 10% of the annual amplitude. The results have been compared with in-situ measurements of the CO_2 flux as well as phenological observations on different test sites, giving RMSE values of 6.3 days and 9.4 days, respectively (Böttcher et al., 2014).

Bradley et al. utilized splines to model the phenology of prairie vegetation in the Great Basin in the United States. With an iterative approach, splines of the order 11 - 14 were used, which have been stabilized by an average annual fit to build a baseline and an upper envelope for the spline. The onset of greening was then assessed using the timing of the half maximum during spring growth as stated by White et al. (1997) and Fisher et al. (2006). The temporal variability of the extracted dates was larger than the spatial variability between different study sites, which led to the conclusion that "similar land cover has a similar phenological pattern in a given year, but year to year phenological variability within a given land cover type may be very high" (Bradley et al., 2007).

Other studies dealt with crop phenology using remotely sensed VI time series, like Cong et al. (2012), Xiao et al. (2013) or Pan et al. (2015). Xiao et al. and Pan et al. found good correlations between satellite- and ground-based phenological stages with a piecewise logistic model (Xiao et al.) and Savitzky-Golay filtering with VI thresholds (Pan et al.). Their studies had been

carried out in well-known regions in China with good statistical reference data (Pan et al., 2015, Xiao et al., 2013). Cong et al. compared five different methods (Gaussian filtering, cubic splines, the HANTS-method, Polyfit and the *TIMESAT*[1] software) for phenology extraction, showing that each model has its own strengths and weaknesses with no "overall best performer" (Cong et al., 2012). This confirms the findings of Mader, who compared a moving average digital filtering method to Gaussian curve fitting and splines. For his study site in China, all three methods have shown consistent results (Mader, 2012).

At the university of Würzburg, Kübert is working on her PhD, deriving phenological information of Germany and focusing on deciduous forests and permanent grasslands. Using a MODIS NDVI time series, the phenological parameters are extracted with the *TIMESAT* software. Reference data are ground based observations from the German Weather Service (Deutscher Wetterdienst) (DWD) as described in Section 2.2, together with own observations from about 300 locations. First results show reasonable spatial patterns for the SOG, but they still need to be evaluated (Kübert, 2015, Kübert et al., 2011).

TIMESAT is an open-source software, developed at the universities of Lund and Malmö in Sweden. It provides the user with a graphical user interface and three different modelling methods to choose from: local polynomial functions, which are classified as adaptive Savitzky-Golay filtering, and two least-squares methods of fitting non-linear functions of different complexity. The data have to be pre-processed to remove outliers and spikes in the time series and the time steps must be equally distributed. Additionally, the time window for the seasonality has to be set and the time series is split into single seasons of that length. The onset of greening is then specified as that DOY, when a user-defined VI threshold is exceeded. Using this threshold as well as the annual maximum and the minima to its left and right, all other phenological parameters (up to 11 different descriptors) are then extracted (Eklundh and Jönsson, 2015).

[1] http://web.nateko.lu.se/timesat/timesat.asp

1.3 Study area and objectives

During his PhD at the university of Trier, MADER developed a framework for the phenological analysis of remote sensing data. He showed, that splines are as suitable as any other method for deriving phenological descriptors from remotely sensed VI time series, while being very easy to use, completely data-driven and without the need of pre-processing (MADER, 2012). He also designed a number of C++-based programs (summarized under the name *splits*), which make it relatively easy for the user to extract phenological parameters from a VI time series. After being tested for a large scale cropping region in the northwestern part of China, the same approach has been applied for Germany in this Master thesis. While the Aksu site in China is very homogeneous, consisting mainly of sand dunes with sparse vegetation on the one and vast, irrigated cotton fields on the other hand (MADER, 2012), Germany is a highly diverse region with all kinds of land use types and ecosystems of different spatial extent. $\sim$ 30 % of the land surface is covered by forest, agricultural areas make up for $\sim$ 52 % (DESTATIS, 2013). But it is not the land use itself, which makes Germany so heterogenous. Agricultural areas are often characterized by changing crops from one field to another (BMBF, 2015), and german forests are highly diverse ecosystems even when they are used for forestry (BMEL, 2014b). Hence, spectral mixing is expected to be a problem, where different, small-scale land use classes are covered by the same pixel and cause a disturbed VI signal.

The aim of this study was to derive phenological descriptors from a MODIS-derived EVI time series, covering the land surface of whole Germany, and to evaluate the results with ground based observations gathered by the DWD. The latter have been made publicly accessible recently and are collected since 1951. To get a time series which is as long as possible, the whole MODIS archive since February 2000 has been used. Though it was clear that the study area is very complex and diverse, which makes it difficult to apply such a general approach for a whole country, the hypotheses were the following:

- With the help of the *splits* framework, it is possible to extract reasonable phenological parameters for Germany, regardless of the land use.
- Spatial patterns of the general land use classes are recognizable from the spatial distribution of these descriptors (e.g. the SOG).
- The phenological parameters are consistent within land use classes and therefore representative for that specific class.

2

Data

2.1 Time Series

MODIS is a key instrument on board of the satellites *Terra* and *Aqua*, orbiting the Earth at an altitude of $\sim 705\ km$ (NASA, 2015a). It collects data in 36 bands at wavelengths from 0.405 to 14.385 μm with spatial resolutions from 250 m to 1 km (NASA, 2015b). These data are automatically processed into a set of products[1], which can be downloaded for free through the respective data delivery system[2].

The time series, from which the phenological parameters were to be extracted, was created with the MODIS VI products *MOD13Q1* (*Terra*) and *MYD13Q1* (*Aqua*), both with a spatial resolution of 250 m. They provide the same datasets, where the two vegetation indices NDVI and EVI, together with their quality flags, are the most important ones. The latter are byte-coded images, indicating a measure of the reliability of each pixel value (LP DAAC, 2014a,b) (for further reading, see the detailed product description on the respective websites[3,4]). The datasets are 16-day composites, which means that an image is assembled by pixels from different dates within a 16-day period. During this time, for each pixel the two dates with the highest respective VI values are stored, from which the one with the smaller view angle is then used for the final product. The information about the acquisition date corresponding to each pixel is stored and delivered as

[1] https://lpdaac.usgs.gov/dataset_discovery/modis/modis_products_table
[2] http://reverb.echo.nasa.gov/reverb/#utf8=%E2%9C%93&spatial_map=satellite&spatial_type=rectangle
[3] https://lpdaac.usgs.gov/products/modis_products_table/mod13q1
[4] https://lpdaac.usgs.gov/products/modis_products_table/myd13q1

a DOY image (Didan and Huete, 2006, p. 5 f.).

From the two available vegetation indices, the EVI was chosen, because, in contrary to the NDVI, it "corrects for some distortions in the reflected light caused by the particles in the air as well as the ground cover below the vegetation" (Meier and Herring, 2000). The latter is an important point when utilizing the best possible VI signal with as few distortions as possible.

2.2 Phenological Data

The DWD provides information about the phenological stages, like blooming, harvesting or leaf fall, of different plants in Germany since the year 1951. These data are collected by volunteers at specific locations during the whole year. It has to be stressed, that every volunteer is free to choose the territory she or he observes and is only recommended (not constrained) to monitor an area with a radius of 1.5 - 2, in some cases even up to 5 km. Additionally, the observed plant species shall be representative for the volunteers territory (DWD, 2012). Hence, there is a high uncertainty within the data, because there is no fixed guideline for the data collection, and the quality and accuracy strongly depend on the volunteers' experience and motivation. This has to be kept in mind when it comes to interpreting the results of the validation.

The data are collected at 6494 phenological stations in Germany, covering the whole country, including many islands, in a (seemingly) random pattern (see right side of Figure 2.1). The geographic locations of all stations can be downloaded as a text file from the DWD's ftp-server[5]. For each plant species, there is a single text file (also downloadable from the respective folder of the same server), which contains all observed phenological stages for each station and year. Table 2.1 shows the first lines of such a text file for Beech. "Quality" is a flag, which indicates different stages of validation (1 means only a formal check at entering). "Station" is the unique station number (ID) and "Year" is the reference year for the following

[5] ftp://ftp-cdc.dwd.de/pub/CDC/observations_germany/phenology/annual_reporters/

Table 2.1: Head of a raw text file as delivered by the DWD, sorted by the station ID, containing the phenological stages for Beech.

Quality	Station	Year	Species	Phase	Entry date	ED quality	Julian day
1	3	1951	123	4	19510502	1	122
1	3	1951	123	5	19510507	1	127
1	3	1951	123	62	19510914	1	257
1	3	1952	123	4	19520429	1	120
1	3	1953	123	4	19530427	1	117
1	3	1954	123	4	19540430	1	120
1	3	1954	123	31	19541101	1	305
1	3	1955	123	4	19550503	1	123
1	3	1955	123	31	19551031	1	304
1	3	1956	123	4	19560503	1	124
1	3	1958	123	4	19580504	1	124
1	3	1958	123	31	19581016	1	289
1	3	1960	123	4	19600504	1	125
1	3	1961	123	31	19611106	1	310
1	3	1962	123	4	19620513	1	133
1	3	1962	123	31	19621102	1	306
1	3	1963	123	4	19630517	1	137
1	3	1963	123	5	19630521	1	141
1	3	1963	123	31	19631026	1	299

"Species" and each phenological "Phase" within that year. Both entries are coded by an integer value, with the corresponding legend also being available on the ftp-server. The "Entry date" is the date when the plant enters the aforementioned phenological phase in the format *YYYYMMDD*, followed by a plausibility flag for that date (1 stands for unobjectionable). The "Julian day" is the same date, but in the DOY format for the reference year.

2.3 Land Cover Data

Since every DWD station does not represent only the vegetation at exactly that coordinate, but for a larger area around it, it can not be taken for granted, that each species listed for that station really is the dominant one. Thus, it is not sufficient to imply that one station is located in a forest just because the respective phenological file contains, e.g., spruce and pine. To overcome this uncertainty concerning the actual land cover at every station, the CORINE Land Cover (CLC) dataset was used. It is available at the website of the European Environment Agency, can be downloaded as a raster file with a spatial resolution of 100 m

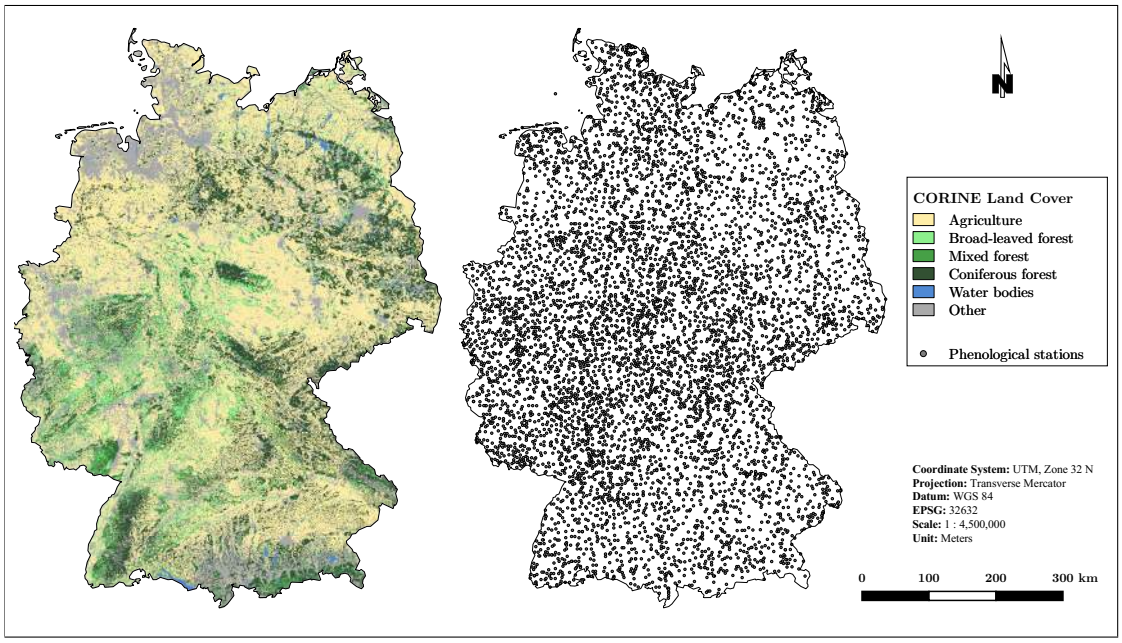

Figure 2.1: CORINE land use map (left) and all phenological stations in Germany (right).

(EEA, 2013)[6] and was chosen over other available land cover datasets due to its very high accuracy and currency, according to Trombik and Hlásny (2013). The dataset has been produced using satellite image interpretation techniques. The basis for the classification, which is the third of its kind (after 1990 and 2000), are the *SPOT-4* and *IRS P6* satellites, with a respective spatial resolution of 20 and 23 m. According to its technical guideline, the dataset has a thematic accuracy of over 85 %, with a minimum mapping unit at ground level of 25 ha (EEA, 2007). Though it does not provide the actual land cover (meaning plant species), it is very useful for distinguishing between the two main land use classes, forest and agriculture. This information has been used to subset the phenological stations according to their respective class (see Section 3.2). Figure 2.1 (left side) shows a reclassified version of the original dataset, where only the main land use classes have been kept, with all others mapped in grey.

The European Commission also provides statistical data on land cover and land use (*LUCAS*) for all member states. The data can be downloaded as tab-

[6] http://www.eea.europa.eu/data-and-maps/data/corine-land-cover-2006-raster-3

ulated files[7], which contain the land use as well as the land cover, in that case the dominant plant species, at the time of the survey. It is repeated every three years since 2006 and is carried out at predefined locations, forming a regular grid of ~ 3 by 3 km. Unfortunately, the coordinates for the survey points do not match those of the DWD stations, which made it impossible to directly match the actual dominant plant species to these locations. Since plant phenology is strongly influenced by small-scale environmental variables such as microclimate, soil moisture or nutrient availability (Bijalwan et al., 2013, Dahlgren et al., 2007, Jackson, 1966), this information was not assigned from the *LUCAS* data to the nearest respective DWD station. Additionally, the problem of the survey's three year repetition cycle would still remain, resulting in suitable references for only these three years. But since the whole time series should be evaluated, it was decided to stick with the more general, but consistent approach of using the CLC dataset, with the assumption of continuity (no change of the land use class at each pixel location during the 15 seasons).

The most important land use classes for Germany are agriculture and forest (DESTATIS, 2013), so the modelling and evaluation of the phenological parameters focused on these two. Forests are very stable, for trees need much time to grow. Therefore, forests do not change their essential species composition over a long period of time. In contrary, agricultural areas are highly dynamic, not only because of the annual cycle of sowing and harvest, but also because their species composition within one field might change not only every year, but sometimes several times over the course of one season. According to the German Forest Inventory[8], the main forest tree species are Beech (*Fagus sylvatica*) and Oak (*Quercus robur*) as deciduous and Pine (*Pinus sylvestris*) and Spruce (*Picea abies*) as coniferous trees (BWI-3, 2012). For agriculture, the most important crops are Maize (*Zea mays*), Barley (*Hordeum vulgare*), Rape (*Brassica napus*) and Wheat (*Triticum spec.*), with the three latter as their respective winter breed (BMEL, 2014a).

[7] http://ec.europa.eu/eurostat/web/lucas/data
[8] https://bwi.info

3

Methods

Besides the programs developed by MADER, the processing of the data was mainly done with self-written scripts in the programming languages *Python* and *R*, to make every step understandable and, more importantly, easily repeatable. Many of these scripts have been written as functions to be reusable and can also be applied to other data. In *R*, functions have been written for drawing grids in plot windows as well as for the comparison of two DOY datasets, which have been used extensively. The most important *Pyton* functions have been developed for downloading data from an ftp-server, layerstacking, spectral subsetting and point and window sampling.

Point sampling is known from *ArcGIS* as the "Extract Values to Points" function or from the "Point sampling tool" plugin of *QantumGIS*. The tool collects raster values at the exact positions defined by an input point-shapefile (see left side of Figure 3.1) and writes those values into the shapefile's attribute table (ESRI HELP, 2012). It also works for multiband-images, creating columns in the attribute table for each respective band. This concept has been reproduced and enhanced in a self-written *Python* script, not only to be able to sample the raster at the exact location indicated by the input points, but also for a window of user-defined size around them (see right side of Figure 3.1). The sampling radius can be set, resulting in a window which is twice the size of this value plus one. The additional pixel comes from the calculation of the window's origin (upper left corner), which is set by using the exact point position and moving as many pixels to the left and to the top as indicated by the desired radius. Hence, only odd-numbered edge lengths for the window are possible (e.g. 3x3, 5x5, etc.). The sampling mode

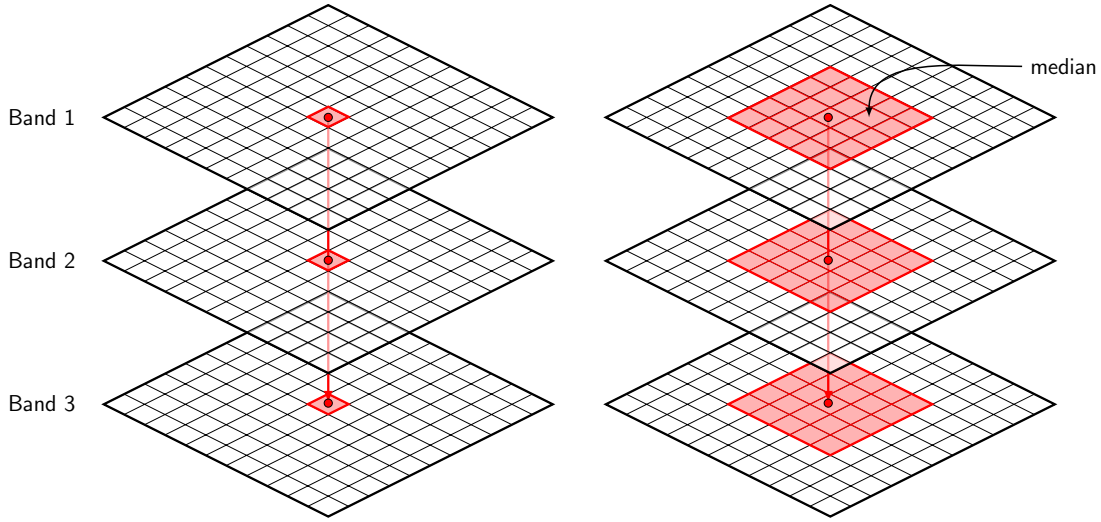

Figure 3.1: The basic concept of point (left) and window sampling (right; window radius = 2).

can be chosen from the options median, mean, minimum, maximum and majority voting. The source code for this function, as well as for all others, can be found online at the author's GitHub-account[1].

The whole workflow is schematically shown in Figure 3.2. There, right-angled rectangles represent raster data, the rectangle with round corners is the DWD text files, ellipses show shapefiles and the tube-like rectangle stands for the statistics and plots for the outcomes of the evaluation. The single steps will be described in the following.

3.1 Time Series

The raw MODIS data have been downloaded from the NASA's data delivery system[2] and all EVI bands were stacked to build a single image containing the whole time series. This was done using a tool called *modis-prepro*, which has been developed by research assistant David Frantz[3] at the "Department of Environmental Remote Sensing & Geoinformatics" at the University of Trier. The tool does not

[1] https://github.com/s6hebern/scripts
[2] http://reverb.echo.nasa.gov/reverb/#utf8=%E2%9C%93&spatial_map=satellite&spatial_type=rectangle
[3] https://www.uni-trier.de/?id=27071

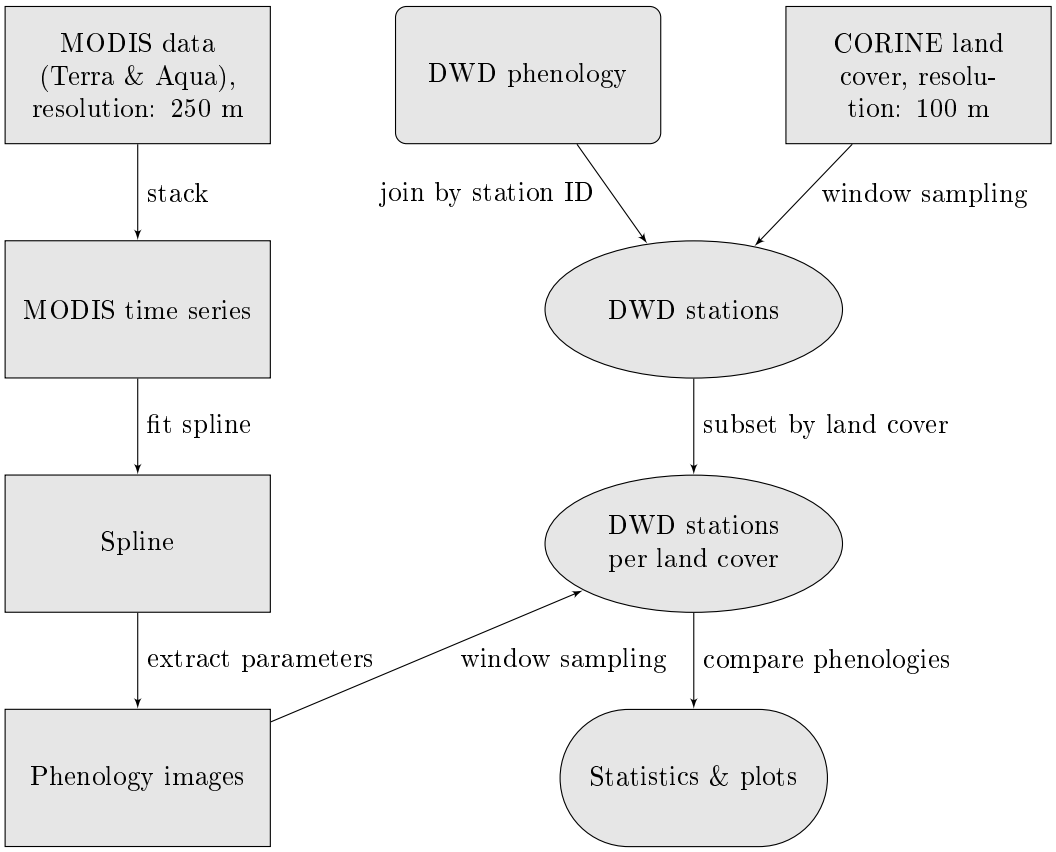

Figure 3.2: Schematic overall workflow.

only create a stack of all available EVI bands, but also of the quality flags and DOY images, only taking the raw MODIS files as input. While data from the *Terra* satellite are available since February 24^{th} in 2000 (LP DAAC, 2014a), the *Aqua* archive starts at July 4^{th} in 2002 (LP DAAC, 2014b), and its 16-day interval is shifted against *Terra* by eight days (LP DAAC, 2014a). Thus, the time series has unequally distributed time steps, theoretically with increments of 16 days until the availability of Aqua and eight days since then. That would be the case, if each pixel from a specific EVI image would have been acquired at the same day. But since the data are 16-day composites, each pixel, containing a complete time series, has its own, irregular time axis, always depending on the respective achievement days. Thus, it was impossible to use the very common tool *TIMESAT* to extract the phenological parameters, because for this, equally distributed time steps are necessary (Eklundh and Jönsson, 2015, p. 41). It then would deal with the

EVI images only, using the center date of the 16-day-composite as the timestamp, which would lead to a wrong time axis for each respective pixel. Instead, the *splits* framework uses the DOY images to supply a correct time axis for every pixel, without relying on a global one.

3.1.1 Splines

Once the time series was complete, an appropriate spline curve had to be fitted. Basically, splines are piecewise polynomials, which make up a function to represent or approximate a set of points. The concept describes the idea of forcing e.g. a straight wooden lath to bend by using several clamps (see Figure 3.3). This can be translated into mathematics by interpreting the clamps as vectors, which are connected (or approximated) by a set of polynomial functions (Mader, 2012). These polynomials are tied at so called "knots" and maintain the continuous nature of the spline function (Prautzsch et al., 2002). Following the basic theorem of de Boor (1972), the number of knots, which is one more than the number of polynomial pieces, controls the smoothness of the spline curve (Faraway, 2006). Given that, a basic, non-smoothing spline model with a number of knots equal to the number of data points will result in the exact representation of the original data. Many different sorts of splines have been developed over the years, each of them with different optimization criteria, constraints and properties. The aforementioned *splits* framework developed by Mader supports B- and P-splines with different smoothing criteria to choose from (Mader, 2012, p. 87 f.).

Besides the type of the mathematical function, the main criterion for the assessment of plant phenology from a time series is the determination of the value for the onset of greening. It can be extracted from the modelled curve using the inflection points (Soudani et al., 2008), changes in curvature (Zhang et al., 2003) or a VI threshold. For the latter, each VI value within one year is converted into a ratio between 0 (for the annual minimum value) and 1 (annual maximum). The growing season begins when the VI value exceeds that threshold (White

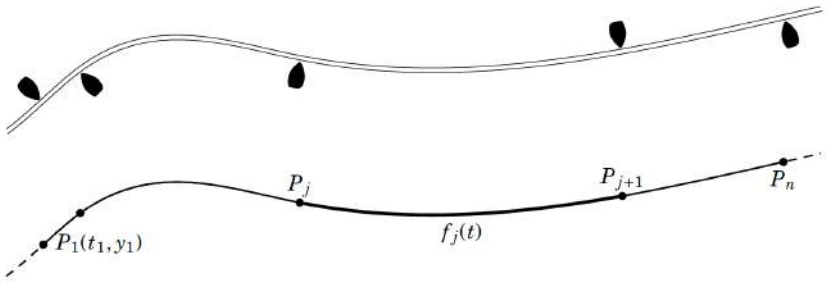

Figure 3.3: The basic concept of splines, with a craftmen's spline at the top and its mathematical equivalent at the bottom (MADER, 2012, p. 35).

ET AL., 1997), where BRADLEY ET AL. stated, that a value of 0.5 "is stable and consistent across ecosystem" (BRADLEY ET AL., 2007). This approach is used in the *splits* framework, where the threshold is called "greenness parameter" (g) and can be chosen by the user.

3.1.2 The *splits* framework

Splits consists of four components with different tasks, in- and output variables. *Splview* (1) is the data viewer, allowing the user to examine the time series visually. Most importantly, a spline curve can be set up by choosing from different splines and a variety of options (see Figure 3.5). That spline is then fitted to the whole time series dataset by *splfit* (2), which creates a new image containing the coefficients of the chosen spline for each pixel. With *splcal* (3), it is possible to create a modelled version of the original time series according to these coefficients for further analysis or prediction purposes, but this function was not used. Finally, *phencal* (4) extracts the phenological parameters from the spline representation of the time series given by the coefficients and creates the respective output files. The algorithm searches the full time series for the global maximum and then places a grid with a window size of one year (because a growing cycle is assumed to have a length of one year) over it, ranging half a year to each side. By this, the growing cycle becomes independent from the calendar year and only relies on the position of the global maximum. For every window, the algorithm then determines the

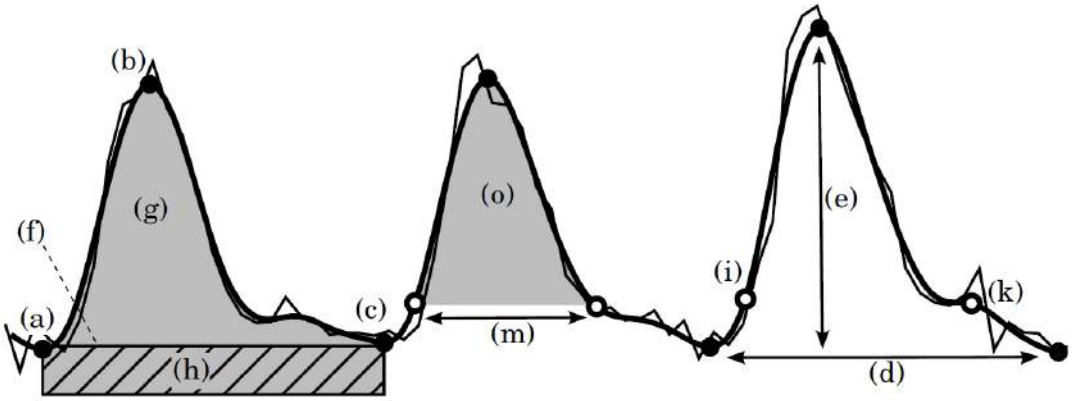

Figure 3.4: All phenological parameters that can be extracted with *phencal* (MADER, 2012, p. 64).

respective maximum as well as the early and late minima (to the left and right of the local maximum). They make up the growing season, from which all other phenological parameters are extracted (MADER, 2012). There are 20 different descriptors (see Figure 3.4), from which only the SOG and end of greening (EOG) (i and k), the greenness duration (m) and the amplitude (e) have been used in this study. A full list of all extractable parameters with the respective descriptions can be found in the PhD-thesis of MADER (2012, p. 64 & p. 91 f.).

3.1.3 Fitting the spline

Following that framework, *splview* was used to display the data and to choose a spline curve which represents the temporal development of the EVI best without losing too much information due to smoothing. Figure 3.5 shows the *splview* main window and one band of the time series (15^{th} of April 2014 as the center date of the 16-day composite). In the upper part, all EVI values at the marked pixel location (red cross) for the whole 15-year timespan can be seen (thin black line), together with a spline curve of 55 knots (bold black line). The green vertical lines mark the "skeleton", meaning the breaks for each year as given by the DOY image, which marks the timeline. The small dots on the spline curve show the seasonal minima (hollow grey dots) and maxima (filled black dots). The small window to

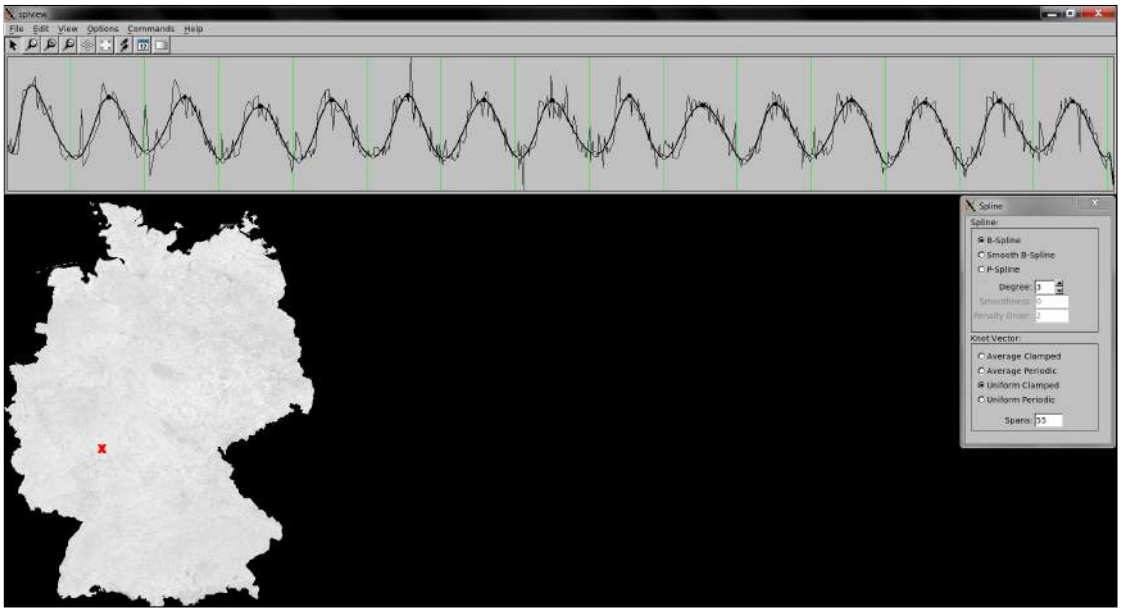

Figure 3.5: A screenshot of the *splview* main window, showing the study area, the time series at the marked location (red cross) and the spline curve with the properties displayed in the box to the right.

the right allows for the adjustment of the spline, giving the user full control over its type and degree as well as the number of knots (called "spans" in here) to use.

Due to the fact, that each pixel within the time series file shows a unique EVI curve during the nearly 15-year timespan, there can be no perfect function which represents all pixels equally well. Therefore, it was decided to visually inspect different regions with distinct land use types and then take the spline which seems the most suitable compromise. In this case, a uniform clamped B-spline with 55 knots (for the 633 steps which made up the whole MODIS time series) was used. More knots would result in a rougher, less knots in a smoother curve, which both did not seem appropriate. Figure 3.6 demonstrates the effect of changing the number of knots. The grey solid line in the background is the original time series (shortened to the year 2007). In the foreground, three different spline curves are shown: one with 55 knots (black line), which was actually used, and two others (red lines) with fewer and more knots. As the plot shows, few knots lead to a very smooth curve, loosing even the seasonality, while using more knots traces the original data more precisely, but results in a stronger influence of extreme values

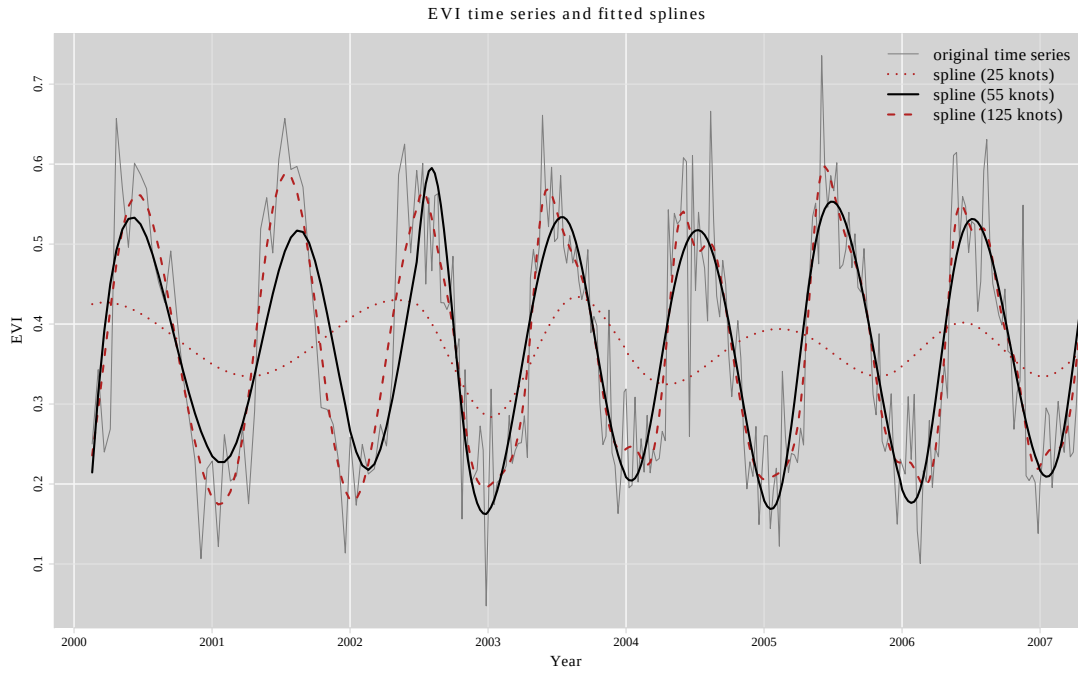

Figure 3.6: Three spline curves with different numbers of knots, fitted to an example EVI time series (mixed forest). The spline represented by the solid black line was used for the actual analysis.

and outliers. Additionally, some features might remain, like the small additional peaks in 2004 and 2006, which may cause troubles in the determination of the growing season.

Splfit was then used to create the image containing the spline coefficients, from which the phenological parameters were then extracted using *phencal*. As mentioned above, for that step the greenness parameter g is crucial, because it defines the threshold (percentage of the annual EVI amplitude) for the start, duration and end of greening. Hence, it was decided to use a range of values from 0.15 to 0.85 with steps of 0.05, resulting in 15 different outcomes for each phenological parameter. These descriptors are written into a multiband raster file by *phencal*, where each band represents one of them for each year. Additionally, the program creates metafiles, which make it possible to create raster files containing either all parameters for one year or one descriptor for each year.

Table 3.1: The species, which were used for the analysis, and their corresponding phenological phases.

Species	Phenological phases	Corresponding parameter from *phencal*
Forest		
Beech Oak	Foliation, leaf senescence / colouring	Start & end of greening
Pine Spruce	Sprouting	Start of greening
Agriculture		
Barley Maize Rape Wheat	Sprouting, harvest	Start & end of greening

3.2 Phenological Data

The raw text file from the DWD, containing a unique station ID, the coordinates, names and some additional information of every phenological station, has been converted to a point shapefile for better handling. Then, the ID was used to join each station with the phenological information from the raw files for every species using a self-written *Python* script. It takes the respective text file for each species, searches for every station ID and then assigns the entry date of the desired phenological phase from the year 2001 until 2014 to the shapefile. That procedure was carried out for all of the eight species (four for forest and agriculture, respectively) and the two phenological stages for which reference data are available (SOG and EOG). This resulted in single shapefiles for each plant species and phase, e.g. "Foliation_Beech" or "Harvest_Maize", as indicated in Table 3.1. It shows all species which have been used for this study, together with their respective phenological stages as declared by the DWD, and the corresponding parameter from *phencal*. For deciduous trees, the SOG and EOG represent foliation and leaf senescence. For coniferous trees, the SOG stands for sprouting, but there is no phenological phase indicating the end of the growing season. For crops, greenup starts when the first germlings break through, while the EOG is associated with the harvest. Initially, the "late minimum" was used for this, but the results were very poor and improved significantly after using the EOG.

To include the information from the CLC dataset, a window sampling as described in Section 3 was carried out, with the land cover raster (with a resolution of 100 m) and the stations shapefile. To match the recommended observation radius around the phenological stations ($\sim 2\ km$), the sampling radius has been set to 20 ($20 * 100\ m = 2\ km$), with "majority voting" as the sampling mode. By this, the most frequent land use class within that window could be assigned to each phenological station. As described in Section 2.3, the most important plant species for each land use class have been used for this study, so it was now possible to assume the dominant plant species at each station (Beech and Oak at stations in deciduous forest, Spruce and Pine in coniferous forest and the four main crops in agricultural areas). Mixed forest was left out because of the high uncertainty concerning the actual main tree species. The stations have then been subsetted by each respective species, resulting in single shapefiles for each of them. Thus, it was ensured that only those stations remain which contain the respective plant species within their observation record and match the corresponding land use class (after the window sampling).

3.3 Combining time series and reference data

After the extraction of the phenological parameters from the time series (see Section 3.1.3), each species shapefile was used to combine it with the resulting parameter images. To be able to compare these rasters created by *phencal* (with a resolution of 250 m) with the ground based observations of the phenological data provided by the DWD, again a window sampling has been carried out. The recommended observation radius ($\sim 2\ km$) around the phenological stations was used to set the appropriate sampling radius (eight pixels in that case ($8 * 250\ m = 2\ km$)). This resulted in a sampling window of 17 by 17 pixels and an edge length of 4.25 km. As the sampling mode, "median" was chosen over "mean" due to its better robustness against outliers. The final shapefiles of each species and phenological phase then contained the following attributes:

- a unique station ID
- additional station attributes like name, location and elevation
- the entry date for the respective phenological phase from the DWD data from 2001 to 2014
- the DOY values of the corresponding phenological descriptor from *phencal* from 2001 to 2014

The actual comparison between the modelled DOY values and the DWD reference data was done in *R* with a self-written script. It draws one point in a scatterplot, if the DWD data contain a value for that particular station and year (which is not always the case due to observation gaps). The reference value is used as x and the modelled DOY as y, which creates plots as shown in Figure 6.2. A perfect match would result in a point lying exactly on the one-one-line. This was done for each species and phase for every year and all 15 greenness values.

4

Results

This section deals with the results from the workflow described in the previous chapter. Some additional calculations have been carried out, which will also be explained here. For some statistics and graphics in Section 4.3, the SOG is used as the main phenological parameter, while the EOG is left out. This is due to the fact that coniferous trees have no real phenological descriptor for that particular stage and therefore no reference data is available. The same holds true for other parameters like the amplitude, the maximum EVI value or the integral. Thus, sometimes the greenup date will be the only parameter to be evaluated.

4.1 Spatial patterns

Phencal is able to produce multiband raster files for each phenological parameter, with every band containing that respective descriptor for one year. From these images, maps can be generated, which demonstrate the spatial patterns of the phenology. Figure 4.1 shows the SOG (left) and EOG (right) for Germany in 2013 (the year was chosen arbitrarily), which have been achieved with a g value of 0.5. The colour ramps are contrary to each other, with blue indicating early greenup and late senescence, respectively, and red showing late greenup and early senescence. In both images, there are no clear trends visible, neither a diagonal shift in the greenup date from northwest to southeast due to a more continental climate nor the patterns of differing elevation in the Central German Uplands. For the latter, there are some few exceptions like the Harz region near the center, the Rhenish Massif in the west or the southern part of the Rhine rift valley in the southwest.

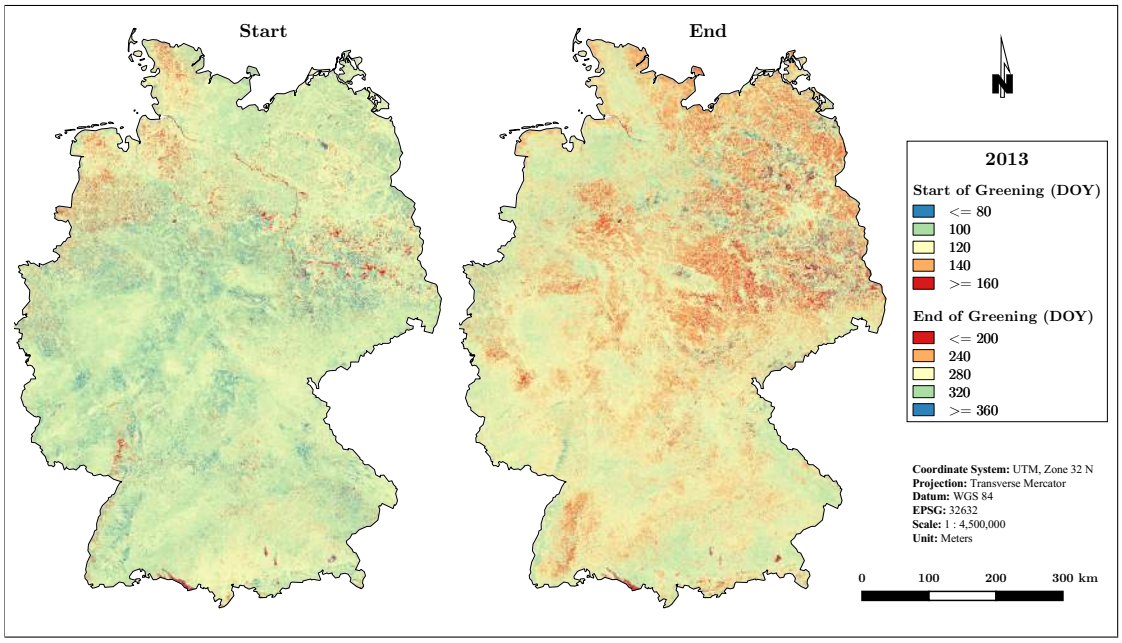

Figure 4.1: DOY maps for the SOG (left) and EOG (right) in 2013.

These areas appear as distinct features with a different colouring compared to their surroundings, but do not necessarily show an influence of elevation.

There are also some small scale structures which are clearly visible, because they differ significantly from their surrounding areas. Big water bodies like Lake Constance and the big lakes near Munich in the south or the Elbe river in the central north can be recognized as distinct red features, especially in the left (SOG) image. While cities and metropolitan areas like the Rhine Main Area, the Ruhr Area or Berlin surprisingly do not stand out, a small, almost linear structure can be seen in both maps northwest of the Rhine rift valley, running from the border of Germany northwards. In the left image, it shows bright red colours, indicating a very late start of the growing season, while changing to blue in the right image, meaning a likewise late end. From a comparison with the CLC dataset, it can be identified as a huge vinicultural area, located at the western slopes of the expiring Rhine rift valley.

One of the hypothesis from the Introduction (see Section 1.3) stated, that the main land use patterns are visible from the spatial distribution of the phenological parameters. As described above, some regions can be identified, while specific

land use classes remain mostly invisible. But from the 20 different phenological descriptors extracted by *phencal*, Figure 4.1 only shows two. Others, in combination with a different way of colouring, might be much more suitable to match the CLC data. Hence, all parameters for the year 2013 have been visually compared to this dataset and the two (seemingly) "best fits" were used for similar maps. The "amplitude" gives the difference between the annual maximum and the EVI base level, which is defined as the mean of the seasonal early and late minimum values. The "greenness duration" is the difference between the SOG and EOG, given in DOY (Mader, 2012, p. 64). These two descriptors can be seen in Figure 4.2 and 4.3 and show the reclassified CLC map (as described in Section 2.3) to the left and the respective phenological parameter to the right. The colour ramps have been chosen to occur as similar to the CLC map as possible for an easier comparison and interpretation. The grey areas in all maps belong to land use classes which are not one of the four main ones and have been mapped on top of the parameter images. On first glance, both descriptors seem to represent the general land use patterns, given by the CLC data, very well. Especially the forested areas in the northeast and east, as well as the agricultural landscapes in the north and center, are clearly visible and even correspond to the colouring of the CLC map. But it is also clear that, despite having different land use classes, for some regions the phenological parameters are very similar. This is particularly obvious in the northwest, where agriculture is dominant. While other agricultural areas show yellowish colours (indicating a high amplitude and a short greenness duration), the compelling colours for this region are lightgreen (intermediate amplitude) and green/darkgreen (long greenness duration). Hence, a classification with these two parameters would presumably result in a misinterpretation of agriculture in this region by assigning some kind of forest instead (and vice versa for other regions). The reason for this has yet to be discovered and may be part of future investigations. Overall, the main land use patterns remain clearly visible, with some exceptions especially in agricultural areas.

For testing purposes, a quick, unsupervised classification was carried out, using

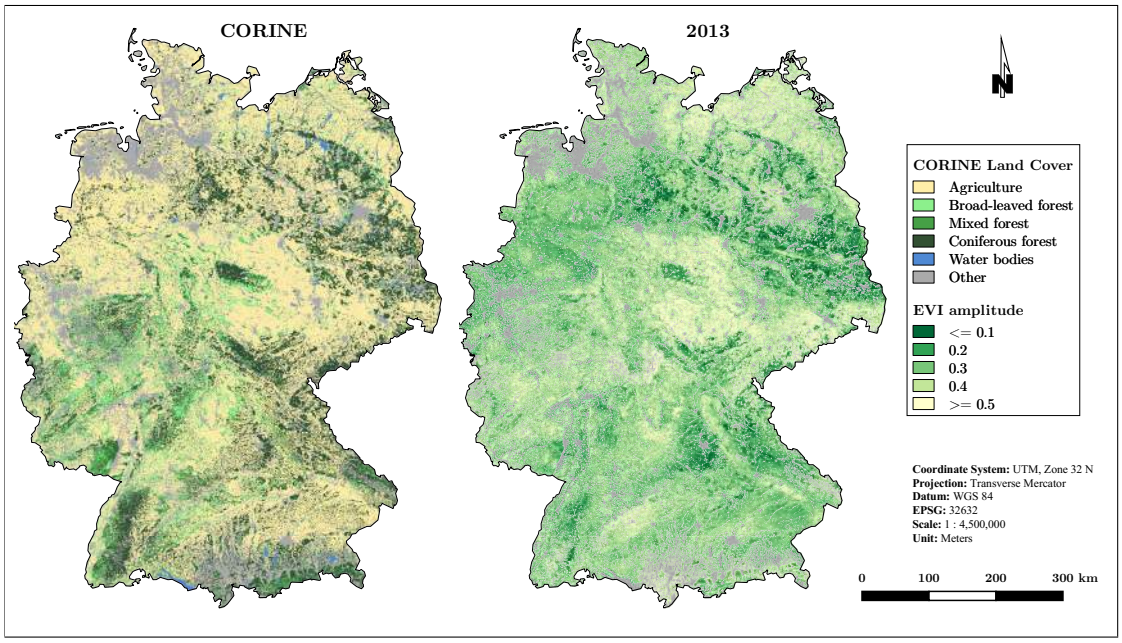

Figure 4.2: Comparison of the CLC dataset (left) with the spatial patterns of the EVI amplitude for 2013 (right).

the *SAGA* tool "Cluster analysis for grids" within *QantumGIS*. It takes a single-band image as an input and assigns a user-defined number of classes, in this case using the *hill-climbing* algorithm of RUBIN (1967). The EVI amplitude for 2013 was used as the input raster to be classified, with four desired classes (deciduous, coniferous and mixed forest together with agriculture, see Figure 4.4). The colour ramp in the legend represents both maps. The classification reveals a very similar outcome as shown and described above, adding to the indication that at least some phenological descriptors reflect the spatial patterns of the general land use classes. The spatial structures remain the same, but the colouring slightly changes compared to the original map of the EVI amplitude. This is due to the fact, that the classification image only consists of four discrete values, to which the respective colours have been assigned, while the amplitude image contains a continuous range of values between zero and one. There, four colours are assigned to distinct values within that range. For all other values, the colours are interpolated, which results in smooth colour transitions rather than the distinct patterns of the classification image with discrete values.

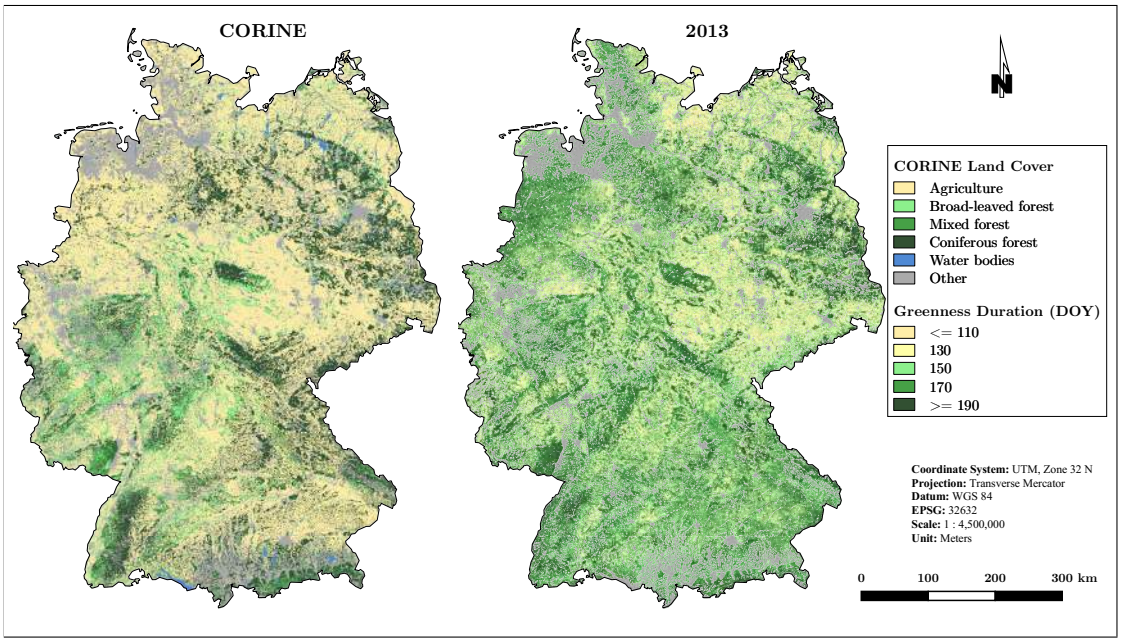

Figure 4.3: Comparison of the CLC dataset (left) with the spatial patterns of the greenness duration for 2013 (right).

Figure 4.5 portraits the histograms for the SOG (left) and EOG (right) for all years, as they are computed and drawn by *QantumGIS*. Each band represents one year, starting in 2001. It is not necessary to distinguish between single bands (years, in that case), but to recognize the many different shapes, amplitudes and even modalities of the curves. Some years show a narrow, more or less symmetric spike (e.g. for the SOG in 2003 (Band 3, blue)), indicating that the respective phenological parameter is within a small value range over the whole image. This means, that different land use classes are difficult to distinguish, because they show very similar values. This can also be seen in Figure 4.7 (which will be described in detail in the following Section), where the values for the SOG in 2003 are slightly above DOY 100 for each land use class. Other histograms are clearly bimodal, like the EOG for the same year. A comparison with Figure 4.7 shows, that the first spike clearly comes from agricultural areas, where senescence takes place around DOY 240 and around DOY 290 for forests. For classification purposes, it is therefore important to either choose the one year with the greatest value distribution or use all years at once (if possible).

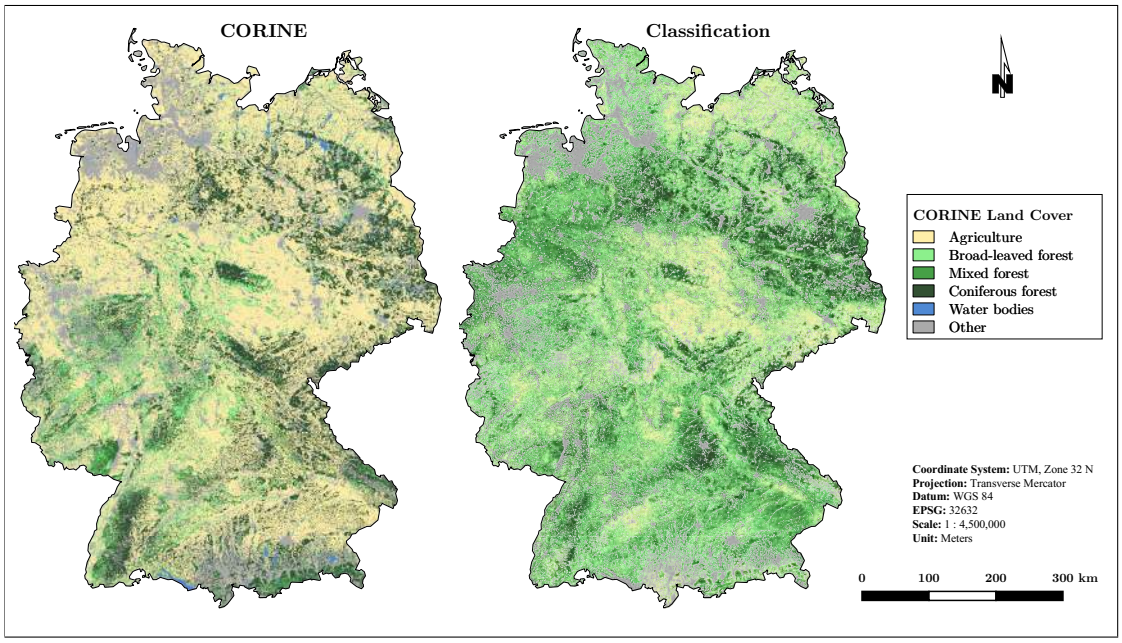

Figure 4.4: Comparison of the CLC dataset (left) with a classification image (right), derived from the EVI amplitude of 2013.

From Figure 4.6, similar findings can be stated. To the left, the histograms for the greenness duration are shown, again with the band number representing the respective year. As seen previously in Figure 4.5, some years show very narrow, symmetric distributions, while others have a bimodal shape or saddle points. Interestingly, the greenness duration reflects the spatial patterns of the main land use classes better than the SOG and EOG (see Figure 4.1). The reason might be, that the greenness duration basically combines the two parameters by showing their difference and therefore enhances distinctions within the respective single parameters. To the right, the amplitude histograms are shown. They all look very similar, forming seemingly normally distributed curves with a wide value range and therefore high standard deviations. This shape might be the reason for the relatively good performance in reflecting the land use patterns, in contrary to high and very narrow spikes, which would lead to maps with much less differentiation (compare Figure 4.1 and Figure 4.2).

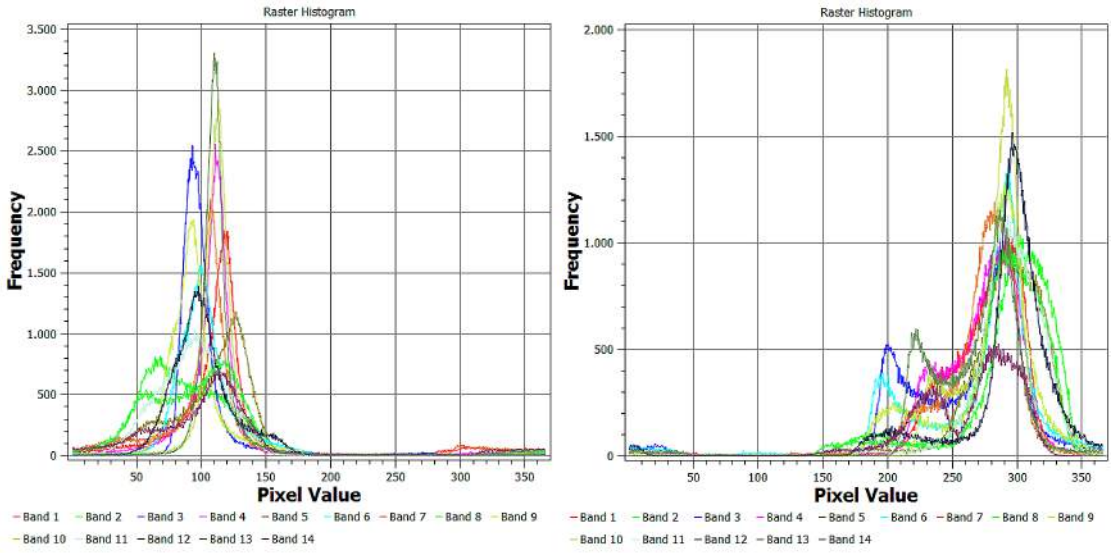

Figure 4.5: Histograms for the SOG (left) and EOG (right) for all years.

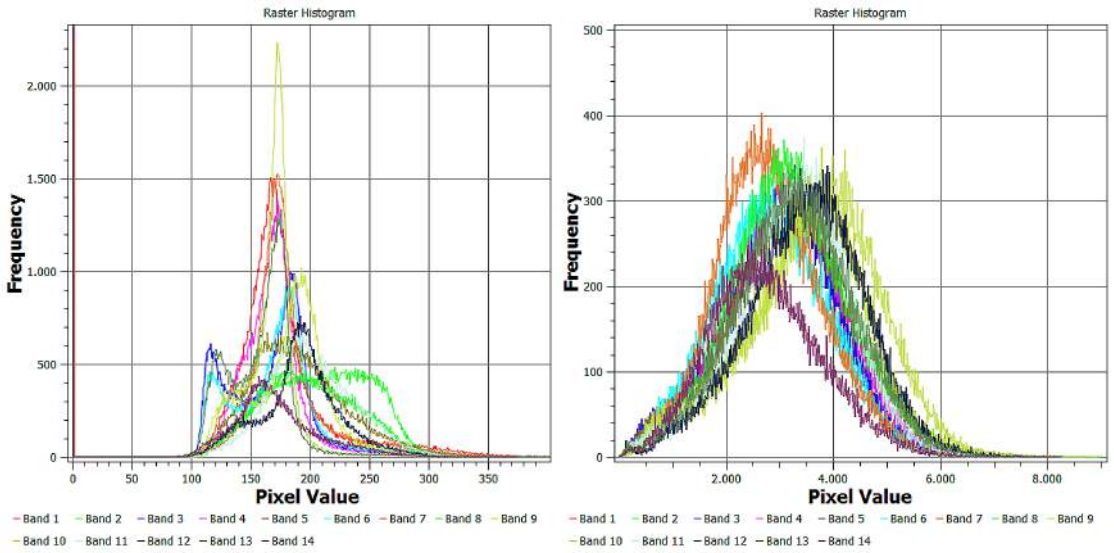

Figure 4.6: Histograms for the greenness duration (left) and amplitude (right) for all years.

4.2 Consistency

To test the consistency of some of the phenological descriptors during the time series within respective land use classes, annual averages have been calculated. This was done using the "Zonal Grid Statistics" tool from the *SAGA Module Library*, which is accessible through the *RSAGA*-package in *R*. The tool calculates

basic statistics of a raster with continuous data (the images with the phenological parameters, derived with a g value of 0.5) within so called "zones", which are defined by a zonal grid with discrete class values (the CLC dataset) (WICHMANN, 2005). By this, statistics like the mean value of the respective parameter become available for every land use class. Figure 4.7 shows the annual means for the SOG (bottom) and EOG (top), encompassed by a band with the width of ± 1 standard deviation, for the three main land use classes over the whole timespan. Furthermore, the mean temperature in April has been added to the plot to check for a correspondence between the greenup date and the temperature in spring. April has been chosen, because the season starts mainly around DOY 110, which is in mid April. The climate data also came from the DWD and can be downloaded from the corresponding ftp-server[1]. Gridded monthly mean airtemperatures have been used and were also processed using the aforementioned *RSAGA* tool to calculate the mean value for each land use class.

From this image, it is very obvious, that different land use classes vary in terms of their phenological parameters. This confirms the findings described in Section 4.1, where maps of the phenological descriptors showed similar spatial patterns as the CLC data, indicating different land use types. Overall, the modelled DOY values for the SOG and EOG of forests look more or less stable and consistent during the 15 year timespan, with the curve for deciduous forest being a bit more ragged than for coniferous forest. The latter reaches its greenup dates slightly later (around DOY 118 compared to 110, according to Table 4.1) and has an overall more or less consistent standard deviation, while deciduous forests vary strongly from year to year in terms of their standard deviation for the greenup dates. Contrasting this, the standard deviation for the EOG is consistently very low, while being much higher, but also consistent for coniferous forests. Agriculture shows a completely different behaviour, with the curves being very ragged, but with consistently high standard deviations. The greenup dates differ from DOY ~ 90 to ~ 130, senescence dates from DOY ~ 240 to almost 300. Interestingly, the

[1] ftp://ftp-cdc.dwd.de/pub/CDC/observations_germany/climate/

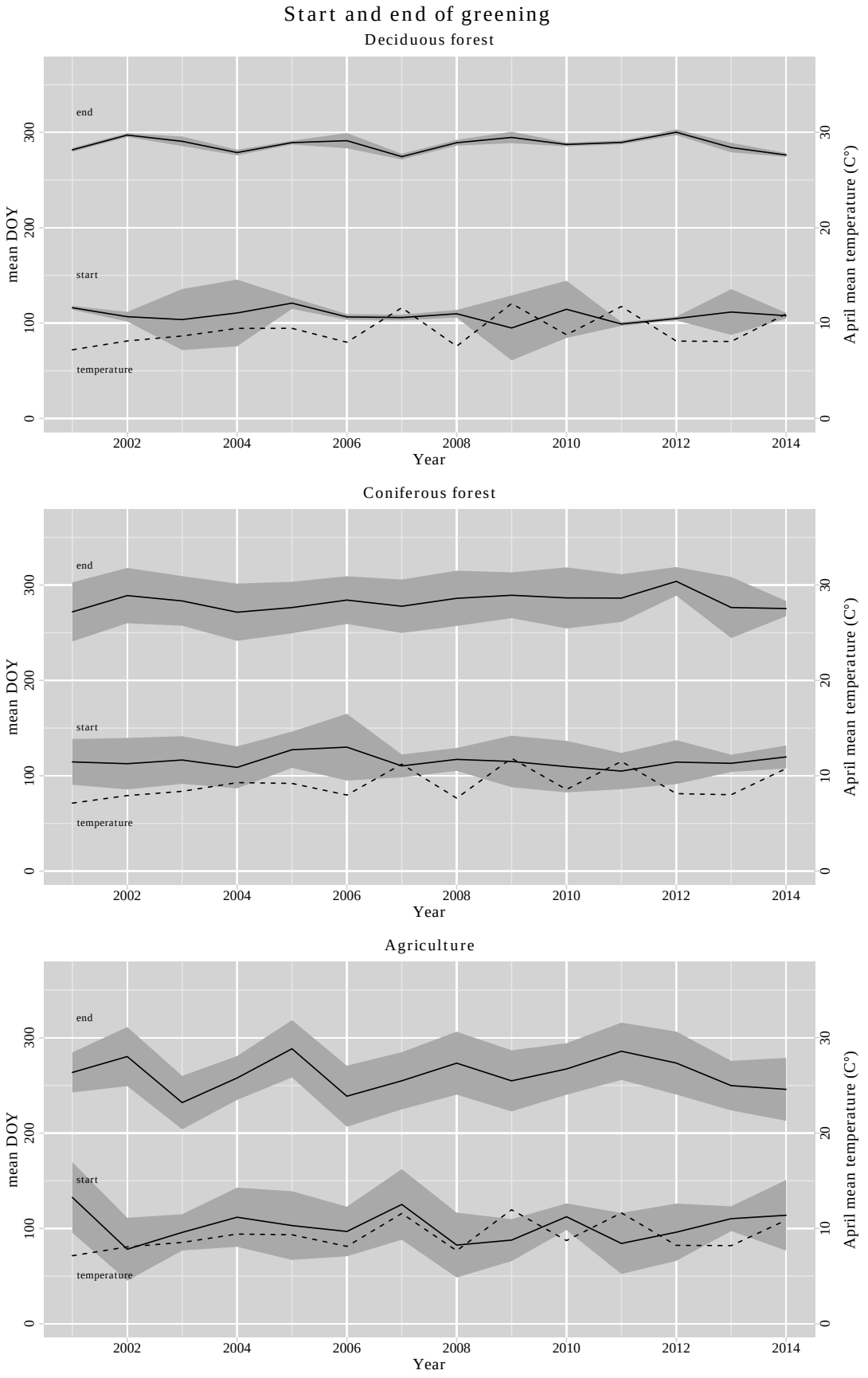

Figure 4.7: Annual means (black line) and standard deviations (grey band) for the SOG (bottom) and EOG (top) depending on the land use class.

curves for SOG and EOG do not have the same shapes and mostly are not even similar, which then would have resulted in seasons of more or less uniform lengths. In contrary, the duration of the growing season differs significantly from year to year, regardless of the land use (but specifically for agricultural areas). Additionally, the monthly mean airtemperature in April only sometimes corresponds to the course of the DOY curves. As described in the literature, so called growing degree days (GDD) can be used to describe and predict phenological events, particularly for cropping systems. The concept of GDD is to calculate a temperature based on the daily minimum and maximum as well as a species-dependent base-temperature, which describes whether a plant is within a stage of activity (meaning growing) or inactivity. It indicates a strong influence of temperature on the plant's phenology and is widely used in agricultural sciences (McMaster and Wilhelm, 1997). Therefore, one might expect a bigger correspondence between airtemperature and greenup date, although the climate data are raw monthly means instead of GDD. In some cases, the effect of a warmer or colder April can be recognized, e.g. for the years 2009 - 2010. There, temperature and SOG mirror each other: when temperatures are high, the growing season starts early, and vice versa. But for other years, like 2004 - 2007, this effect does not show up and sometimes even reverts, e.g. for agricultural areas in 2007.

4.3 Modelled parameters compared to DWD

To compare the phenological data from the DWD with the ones derived from the MODIS time series, scatterplots, similar to those used by Soudani et al., Hmimina et al. or Xiao et al., were created. They contain the DOY for the SOG and EOG for each species, except for the coniferous trees (which have no phenological indicator for the latter phase). Each point in these plots represents one phenological station from the respective land use class as indicated by the CLC raster, where this species should be present according to the DWD data (see Section 2.3). The DWD reference is shown on the x- and the modelled MODIS-

derived parameter on the y-axis, while the one-one-line is shown in grey. The further a point is away from that line, the greater the difference is between the modelled and the reference DOY value for that particular point. The results have been achieved using a greenness parameter g of 0.5, as recommended by BRADLEY ET AL.. Scatterplots for two other g values (0.2, which is the default value in *splits*, and 0.8 to contrast it) can be found in the Appendix for further comparisons. Here, all tree species as well as Maize and Winterwheat are presented (see Figure 6.2 - 6.12).

The plots basically show the same structure: the points representing SOG (green) and EOG (brown) for each respective plant species are clustered in more or less circular-shaped point clouds near or around the one-one-line. Each year looks different, which has already been shown in Figure 4.5. The shapes of the point clouds vary significantly from year to year. While the plots for the tree species show only a small number of points, the point clouds for crops are very big and dense. This is not surprising, because the "agriculture" land use class is much more abundant in the CLC dataset than "forest". Since forests, as well as rural areas, in Germany are often surrounded by arable land, the most common land use sequence in Germany is "rural" - "agriculture" - "forest". The DWD data are collected by volunteers, who choose their territory more or less by themselves and therefore, presumably, close to their homes, which places the phenological station either in rural or agricultural areas. This leads to an over-representation of agriculture over forest when subsetting the shapefiles by their respective land use class and thus, to bigger and denser point clouds. Additionally, the reference data often show observation gaps for single or multiple years. Hence, this date is not compared with the modelled DOY and therefore does not show up as a data point in the image.

Significant differences can be found when comparing the plant species to each other. Not only the total number of points differs, but also the shapes and densities of the point clouds. For Beech and Oak, the points align nicely close to the one-one-line, indicating a good fit between the modelled SOG and EOG and the reference

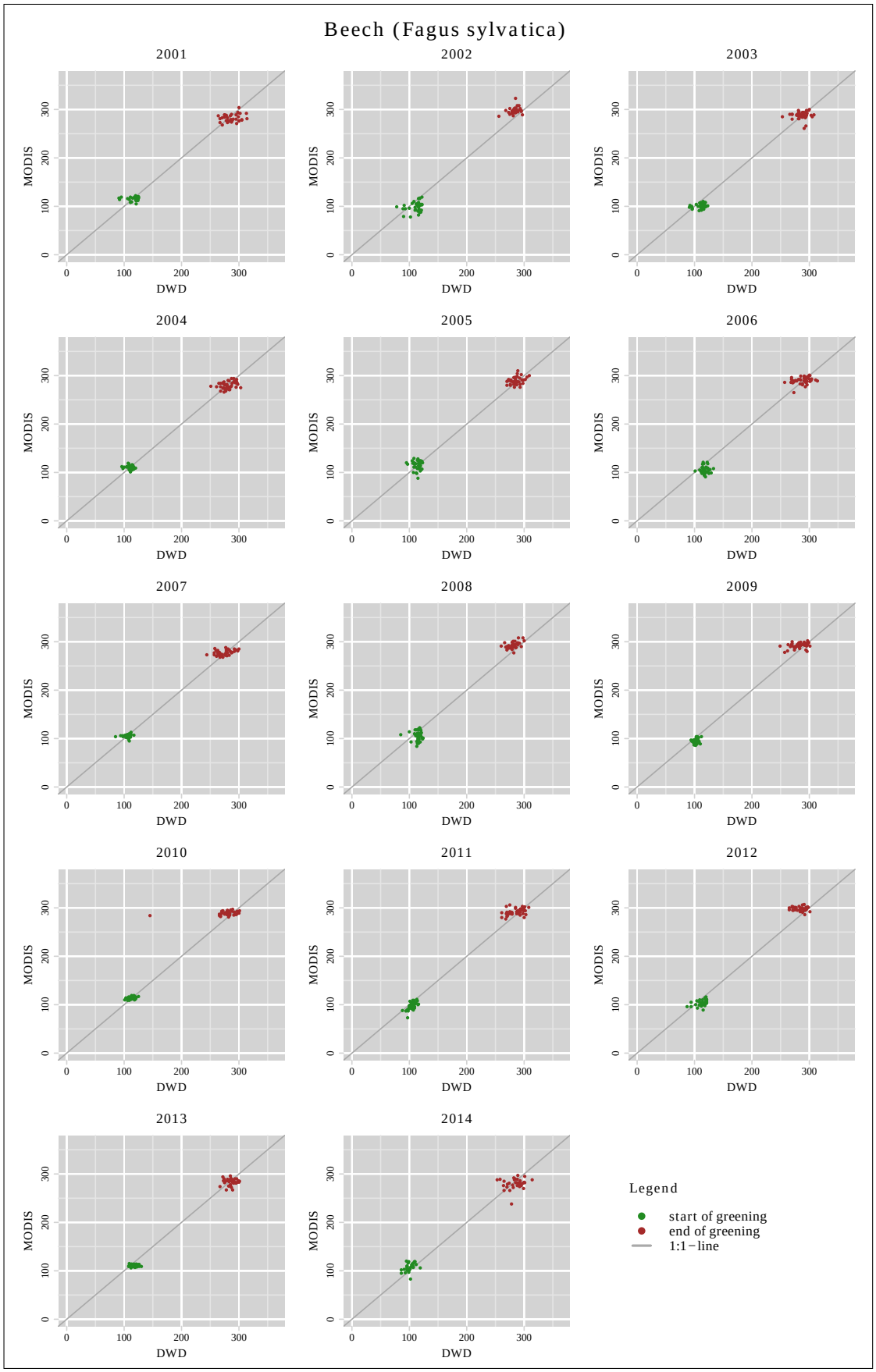

Figure 4.8: DOY comparison for Beech (*Fagus sylvatica*).

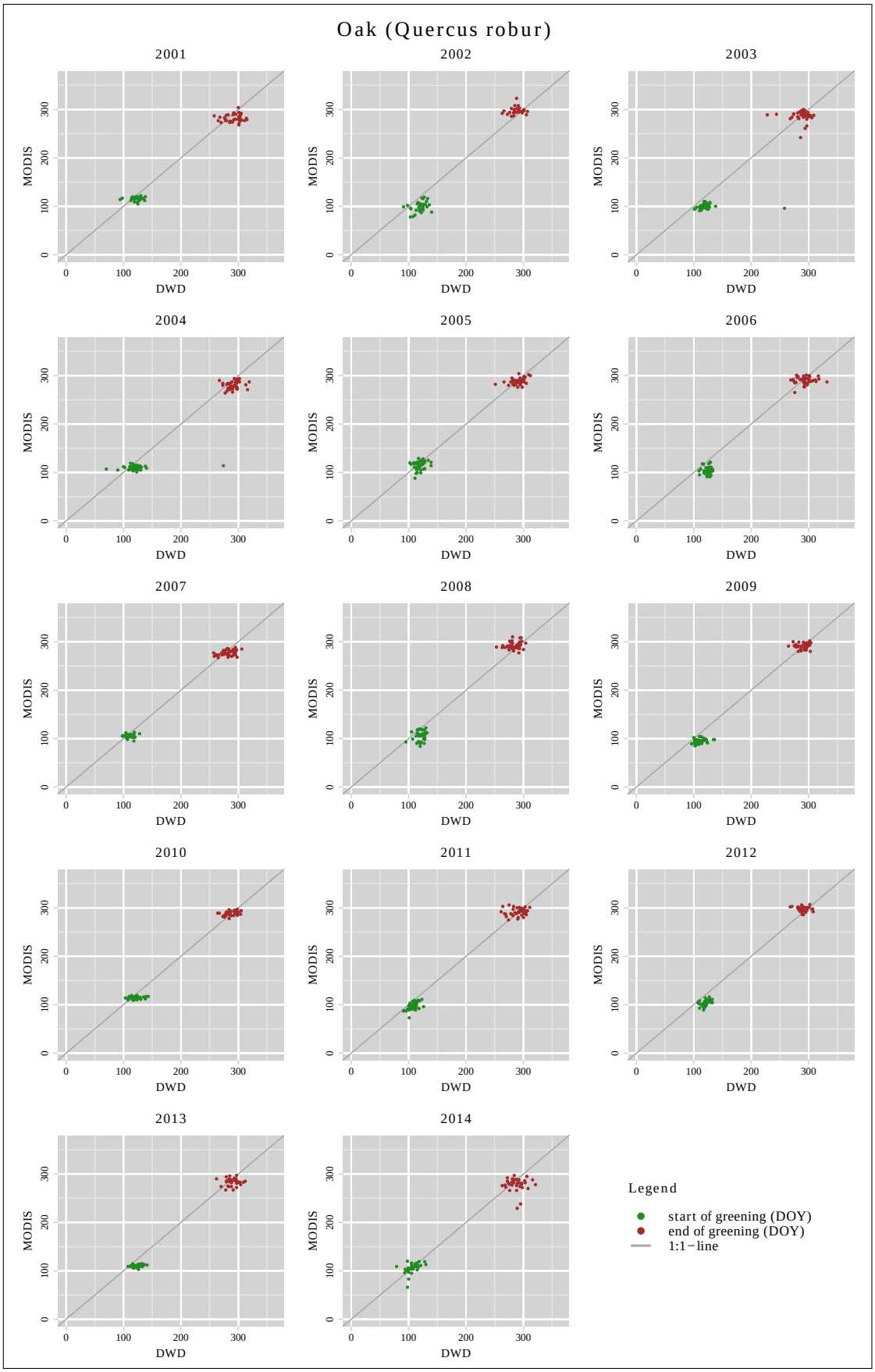

Figure 4.9: DOY comparison for Oak (*Quercus robur*).

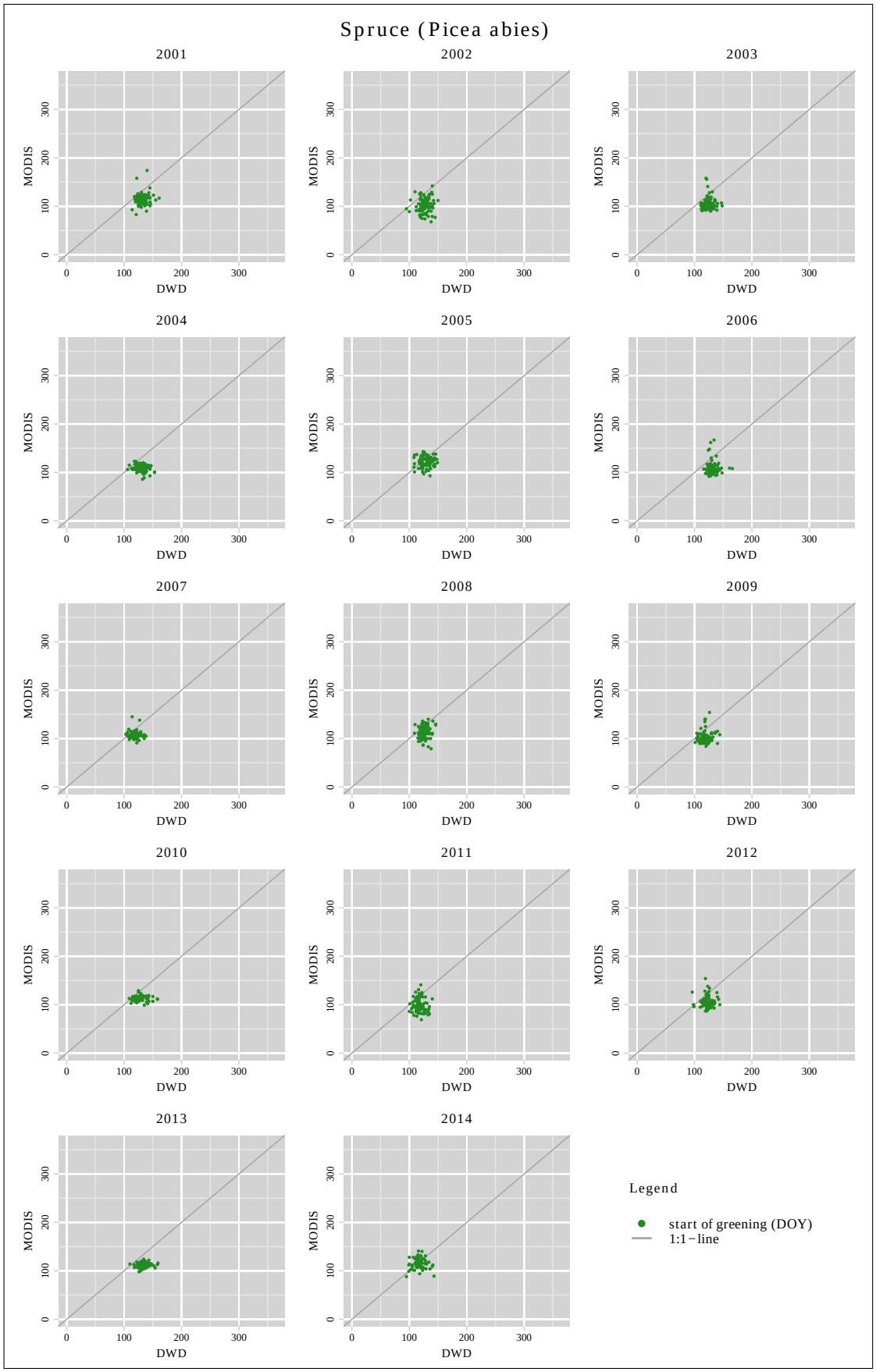

Figure 4.10: DOY comparison for Spruce (*Picea abies*).

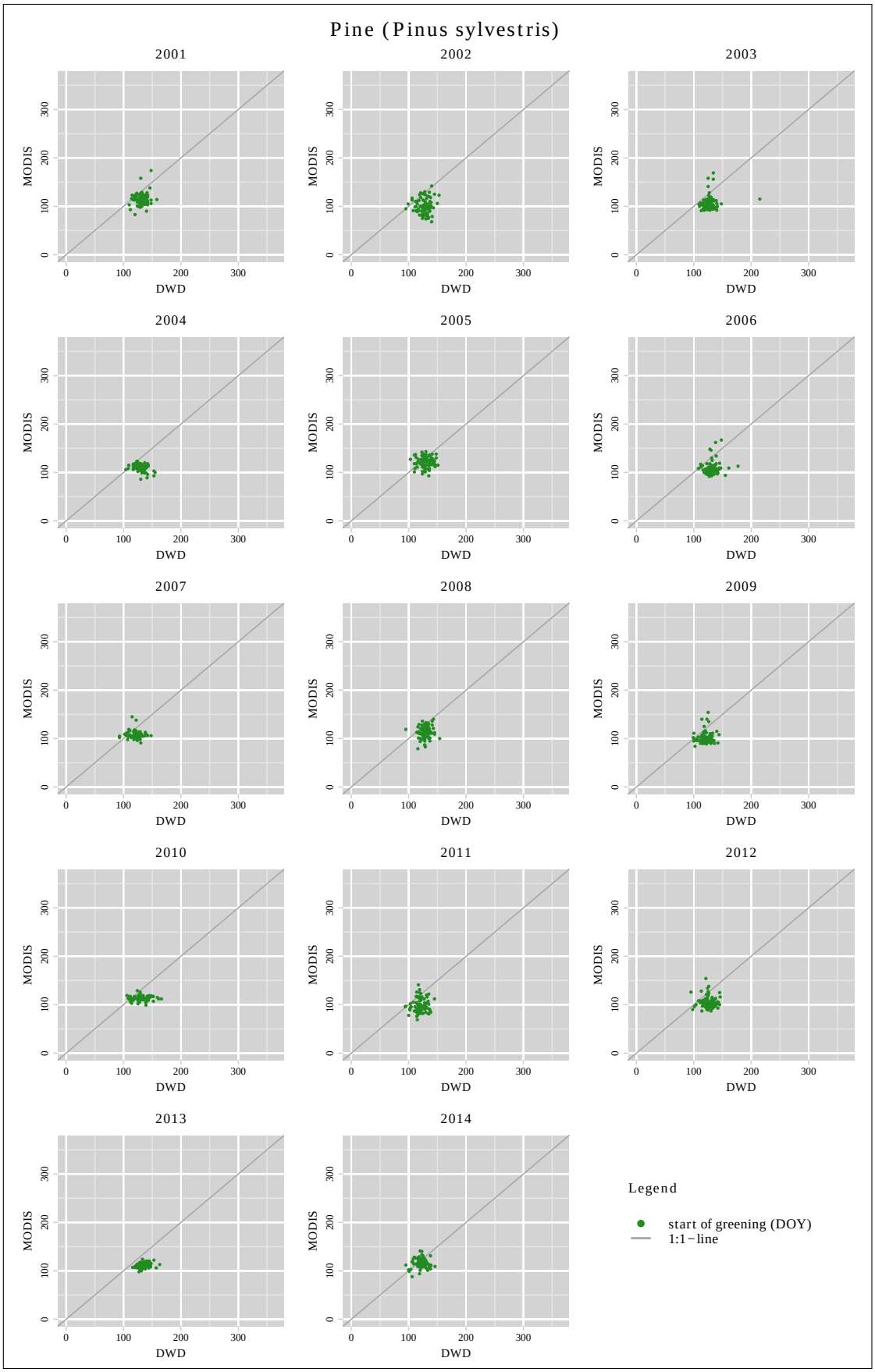

Figure 4.11: DOY comparison for Pine (*Pinus sylvestris*).

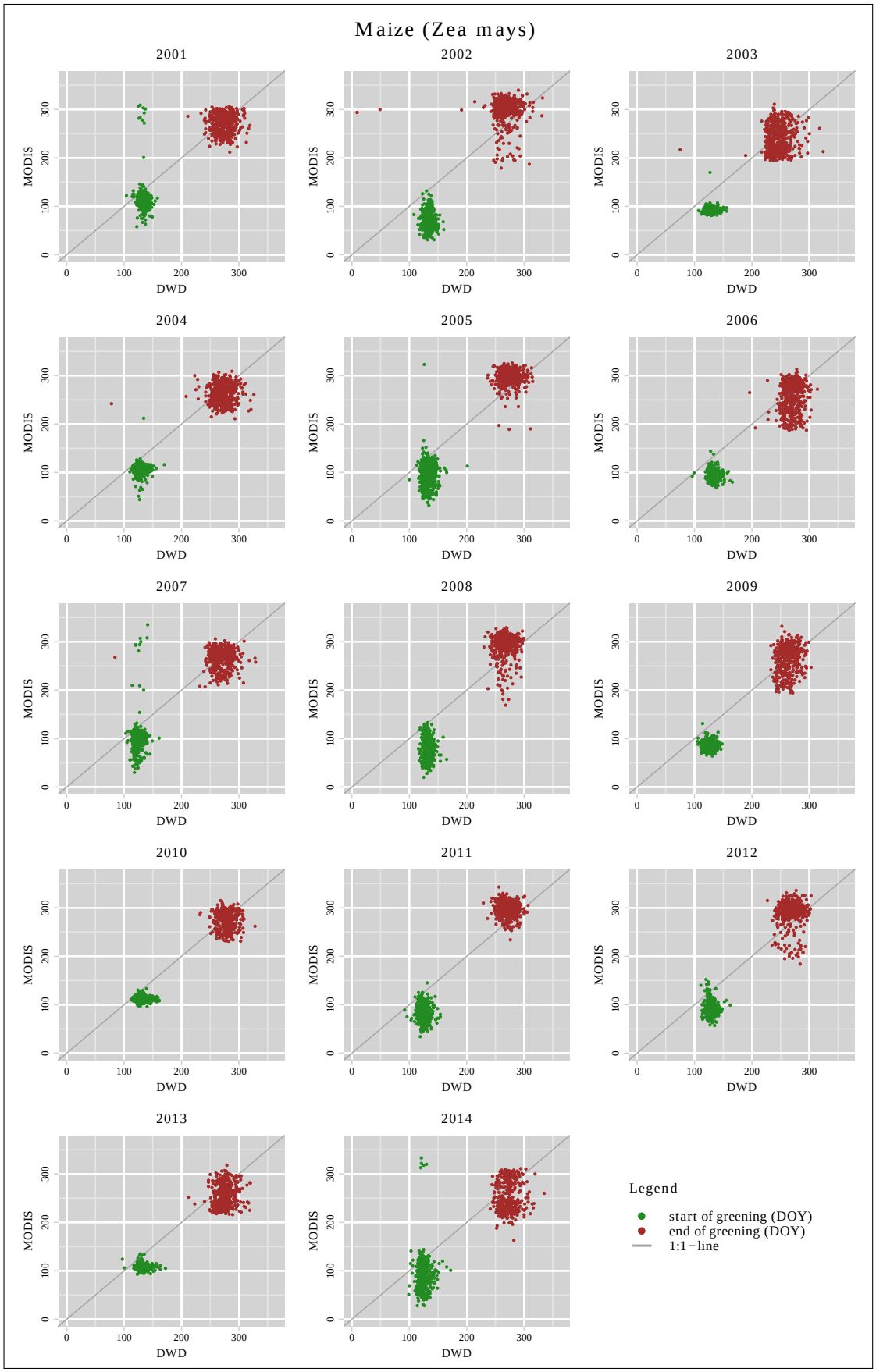

Figure 4.12: DOY comparison for Maize (*Zea mays*).

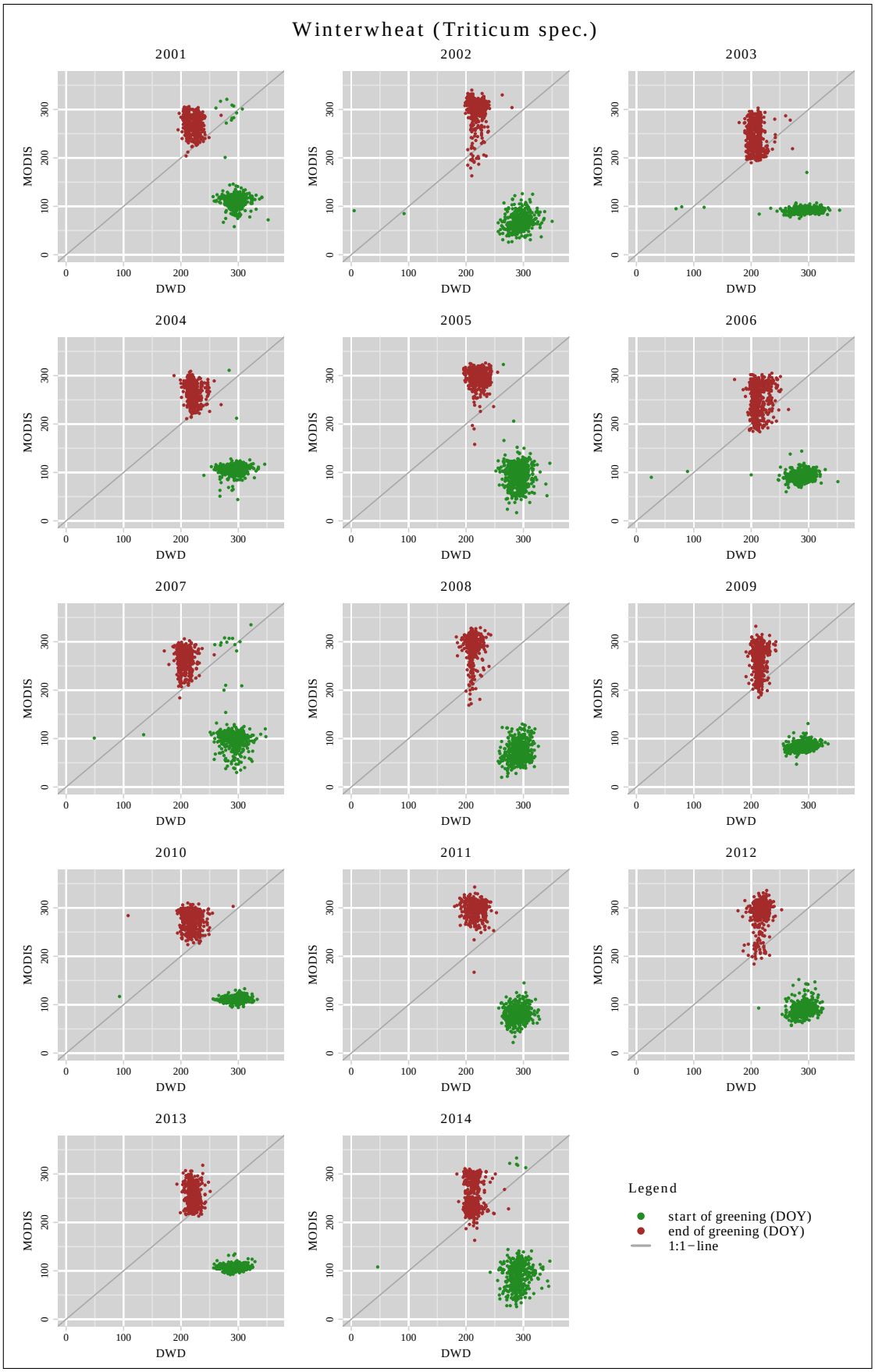

Figure 4.13: DOY comparison for Winterwheat (*Triticum spec.*).

data. Spruce and Pine look similar, despite the fact that there is no phenological marker for the EOG and therefore only one point cloud. In contrary, Maize and Winterwheat show huge point clouds with a lot of scattering. While the points for Maize align very closely to the one-one-line, the parameters for Winterwheat do not fit at all. The point clouds for the EOG are located above the reference line and are mostly stretched in y-direction, indicating a very high variability within the modelled values. For the SOG, the point clouds are located even further to the right and therefore later in time, which would mean that the growing season ends before it has even started. This is due to the fact, that winter crops are sowed in autumn, sprout late in the year and can then be harvested earlier in the following summer. Therefore, the plots may be deceptive, because the growing cycle of such crops is shifted against the calendar year, and the reference SOG of one year actually belongs to the previous one. Obviously, the MODIS-derived SOG dates do not represent this, which will be discussed in more detail in Chapter 5. The other two winter crops show the same patterns, which is why all winter crops are from now on excluded from any further analysis.

4.4 Varying the greenness-parameter

As mentioned above, different values for the crucial greenness parameter g have been tested. Figure 4.14 shows the comparison of the SOG and EOG for DWD stations with occurrences of Beech for three different g values. The respective point clouds for SOG (left) and EOG (right) are connected by the dotted "connection lines" for better visualization.

The comparison reveals a seemingly uniform relation between g and the vertical location of the point cloud. The lower g, the steeper is the connection line, which means that the modelled growing season starts earlier and ends later. For higher g values, the point clouds are pushed towards the vertical center and the connection line flattens. While a g of 0.5 seems to result in a good fit, very high and low values create a season that is too long or too short, respectively. Additionally, the point

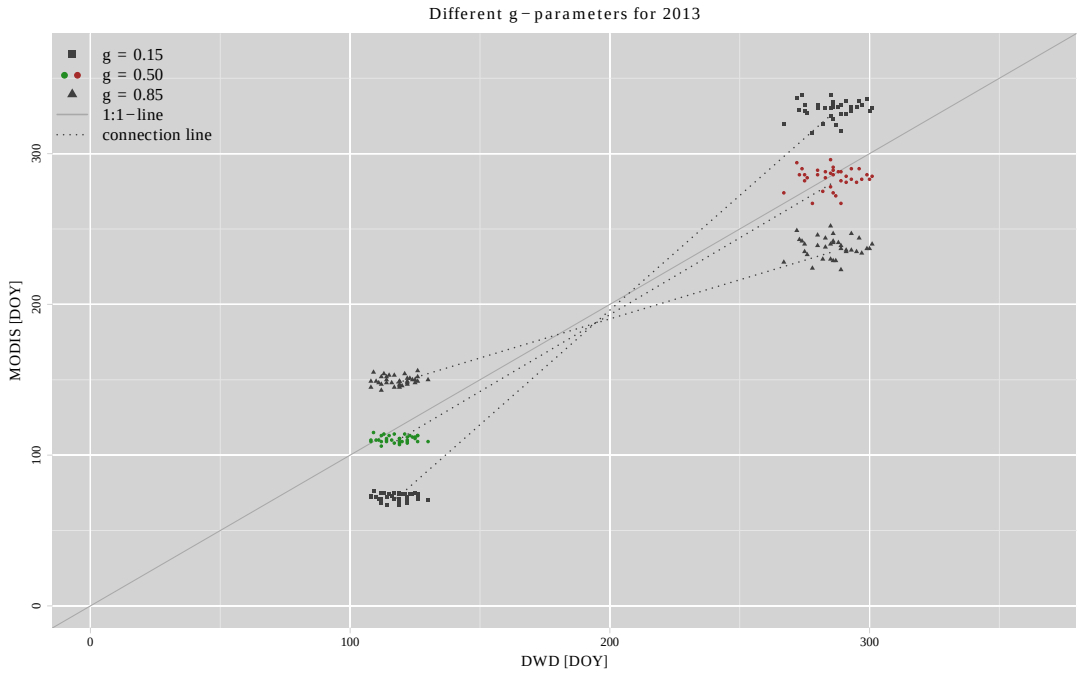

Figure 4.14: Three different values for the greenness parameter g in 2013 for Beech (*Fagus sylvatica*). Points to the left represent the SOG, points to the right show the EOG.

clouds change their shape just marginally and do not move in x-direction, since x is given by the reference data and is therefore fixed. Changing g only moves the point clouds in y-direction: with increasing g values they move upwards for the SOG and downwards for the EOG, creating continuously shorter growing cycles.

To find the most suitable value for g, the median orthogonal difference of the points from the one-one-line has been calculated for the SOG for each g value for all tree species and Maize. If the actual difference between the modelled values and the DWD data would be used, one had to assume unbiased reference data, which does not seem to hold true (see Section 2.2). By using the orthogonal difference to the one-one-line, possible errors in the reference data are taken into account. The results of this calculation are shown in Figure 4.15. Beech and Oak are shown as dots and triangles, Pine and Spruce are represented by the straight and tilted crosses and Maize by the squares.

The trends for all five species are very similar. From the lowest g value (0.15),

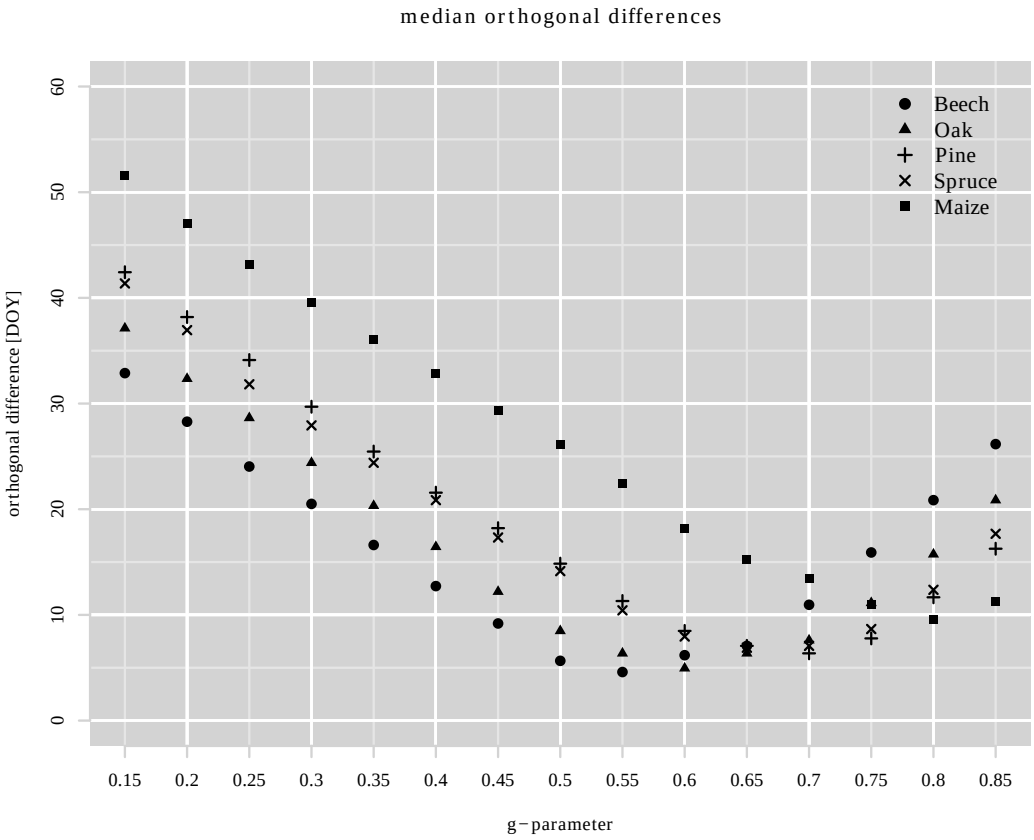

Figure 4.15: Median orthogonal differences for the five main plant species and all g values.

the median orthogonal differences decline from as much as more than 50 days until they reach a species-dependent minimum between 0.55 for Beech and 0.8 for Maize. Beyond that minimum, which is about 5 days at its lowest, the differences increase again, forming a left skewed, u-shaped curve. The two deciduous trees show similar curves for the different g values, with the smallest median orthogonal difference at a g of 0.55 and 0.6, respectively. The coniferous trees are almost identical and show the "best fit" at 0.65 for Spruce and 0.7 for Pine, while Maize reaches its minimum not until 0.8. The image indicates, that the optimal g is not only species-dependent, but is also located at similar values for identical groups of plant. While a medium g produces good results for deciduous trees, high values are needed for good fits with coniferous trees and very high ones for crops.

Table 4.1 shows basic statistics of the point clouds for the five plant species. They have been calculated for the SOG only, but for all different values of g over the full time series. It has to be stressed, that these statistics do not refer to the modelled DOY values, but describe the whole point cloud, including the reference data. "Median" is the median value for the respective point cloud (again, the median has been chosen over the mean because of its robustness against outliers) and "stdv" its standard deviation. "Total difference" is the median of the actual difference between the modelled DOY for the SOG and the reference data, while "orthogonal difference" shows the median of the orthogonal difference (to comprise errors in the DWD data as described previously). Bold numbers indicate the minimum of the respective variable. The table confirms the findings of the graphical representations shown above: a higher g results in higher DOY values for the SOG, while, except for Pine, the "optimal" g (with the lowest (orthogonal) difference to the one-one-line) produces the most dense point clouds with the lowest standard deviation.

As confirmed by the median values of the table, Beeches start their growing season about five days earlier than Oaks. This difference is documented by the reference data, but can not be found in the modelled SOG values (compare Figure 6.2 and 6.4). The point clouds, though showing slightly different shapes, only move in x-direction, which is determined by the DWD data, but not in y-direction (due to the assignment of the respective plant species, see Section 2.3). Coniferous trees also show greater median values, but this time it is recognizable in both directions. With the point clouds for Beech and Oak located slightly below those for Spruce and Pine, it might be possible to separate the two forest types within a classification framework.

Table 4.1: Overall basic statistics of the point clouds for the five main plant species. They have been calculated for the SOG and all g values over the full time series.

g	median					stdv				
	Beech	**Oak**	**Pine**	**Spruce**	**Maize**	**Beech**	**Oak**	**Pine**	**Spruce**	**Maize**
0.15	81.25	86.25	99.25	100.00	114.50	24.13	28.92	31.50	30.72	41.83
0.20	85.25	90.00	100.75	101.75	114.50	20.66	25.55	28.37	27.49	38.26
0.25	91.75	93.50	104.25	104.00	114.50	17.58	22.39	25.57	24.62	34.95
0.30	96.00	97.25	107.00	106.25	114.75	14.86	19.52	23.00	21.91	32.57
0.35	98.25	101.25	109.25	109.75	114.25	12.36	16.86	20.39	19.46	29.31
0.40	102.00	105.25	112.75	112.25	115.75	9.97	14.33	17.87	17.13	26.62
0.45	105.50	108.75	115.00	114.50	117.25	8.08	11.96	15.52	14.89	23.78
0.50	110.00	111.00	118.00	118.00	119.25	7.79	10.39	13.47	12.98	21.42
0.55	113.00	116.00	120.75	120.50	121.00	**6.97**	8.66	11.72	11.23	19.33
0.60	115.75	119.00	123.50	123.00	122.50	7.28	**8.03**	**10.76**	10.57	17.49
0.65	118.75	122.00	127.00	125.50	124.00	8.88	8.22	10.89	**10.49**	15.76
0.70	120.25	125.25	130.00	129.25	125.00	11.20	9.62	11.48	10.92	14.26
0.75	121.75	127.75	133.50	133.00	126.50	13.80	11.85	12.28	12.15	13.45
0.80	123.25	130.00	137.00	135.50	128.50	16.77	14.59	14.24	13.74	**13.16**
0.85	127.00	132.25	140.50	140.00	129.50	19.96	17.75	16.53	16.36	13.54

g	total difference					orthogonal difference				
	Beech	**Oak**	**Pine**	**Spruce**	**Maize**	**Beech**	**Oak**	**Pine**	**Spruce**	**Maize**
0.15	46.50	52.50	60.00	58.50	73.00	32.88	37.12	42.42	41.37	51.62
0.20	40.00	45.75	54.00	52.25	66.25	28.28	32.35	38.18	36.95	47.02
0.25	34.00	40.50	48.25	45.00	61.00	24.04	28.64	34.12	31.82	43.13
0.30	29.00	34.50	42.00	39.50	56.00	20.51	24.40	29.70	27.93	39.60
0.35	23.50	28.75	36.00	34.50	51.00	16.62	20.33	25.46	24.40	36.06
0.40	18.00	23.25	30.50	29.50	46.50	12.73	16.44	21.57	20.86	32.88
0.45	13.00	17.25	25.75	24.50	41.50	9.19	12.20	18.21	17.32	29.35
0.50	8.00	12.00	21.00	19.50	37.00	5.66	8.49	14.85	14.14	26.16
0.55	**6.50**	8.50	16.00	14.50	31.50	**4.60**	6.36	11.31	10.43	22.45
0.60	8.25	**7.00**	12.00	11.25	25.50	6.19	**4.95**	8.49	7.96	18.21
0.65	10.00	8.75	9.50	**9.00**	20.75	7.07	6.36	7.07	**6.89**	15.20
0.70	15.50	10.50	**9.00**	9.25	19.00	10.96	7.60	**6.36**	7.07	13.44
0.75	22.50	15.75	11.00	12.00	15.50	15.91	11.14	7.78	8.66	10.96
0.80	29.50	22.25	16.25	17.50	**12.50**	20.86	15.73	11.67	12.37	**9.55**
0.85	37.00	29.50	23.00	25.00	15.75	26.16	20.86	16.26	17.68	11.31

5

Discussion and Outlook

So far, the raw data, the processing steps and the resulting findings have been described in the previous chapters. In the following, the outcomes will be interpreted and their integration and evaluation in the context of other methods, as described in Chapter 1, will be explained.

5.1 Evaluation of the results

As shown in the previous chapter, the extracted phenological parameters from the EVI time series are overall reasonable and within the expected value ranges. A visual comparison, that some of the descriptors also represent spatial patterns which can be assigned to land use classes as constituted by the CLC dataset. A simple, unsupervised classification confirmed this proposition, showing basically the same structures as the single phenological parameters. A classification algorithm, which can deal with multiband instead of singleband images, would very likely perform much better, making use of the many different descriptors extractable with *phencal* and their respective separability into different classes. Though the median values for SOG and EOG for forests are more or less stable, the overall high standard deviations, especially for coniferous forests and agricultural areas, indicate a lack of consistency within the different land use classes, meaning great variations in the respective parameter's values. The histograms of these descriptors for every single year of the time series also showed a strong variability, which might hint at changing land cover from year to year (except for forest, since they are more or less consistent over decades), e.g. rotating cropping systems. This can

be found in the results of KÜBERT as well, where maps of the SOG vary strongly every year. A correlation between the SOG and the temperature in April could not be confirmed. But this result comes from visual interpretation only, with the monthly mean temperature probably being too general. The concept of GDD, as described by MCMASTER AND WILHELM, might show better correlations when applied consequently and using daily temperature data instead of monthly means.

The two parameters, for which observations from the DWD are available (SOG and EOG), showed good agreements between the modelled values and the reference data, depending on the greenness parameter g. The variation of this crucial parameter revealed, that the optimal value for g is species-dependent and varies strongly. To evaluate the quality of the extracted phenological descriptors, the median orthogonal difference has been used. While good results have been achieved for deciduous forests with g values only slightly above the recommended threshold of 0.5 from BRADLEY ET AL., coniferous forest areas perform best with a g around 0.7. Agricultural areas need even higher values for the "best fit", but still differ strongly from the reference data. Especially winter crops cause big problems, because their season starts in autumn and ends in the following summer. *Splits* should be able to deal with such growing cycles, because it is not bound to the calendar, but in this case it seemingly produced wrong results.

Figure 5.1 illustrates the problem by comparing a "normal" vegetation cycle of Beech (top) with one of Winterwheat (bottom). For the former, the season (dashed black lines) matches the calendar year (grey lines) almost perfectly, with an increase in the EVI (solid black line) in spring, the maximum in summer and a decrease in autumn. Three nicely shaped regular cycles are clearly visible, SOG (grey triangles) and EOG (black triangles) are detected and show up close to the DWD reference data (dots). In contrary, Winterwheat is sowed in autumn, where it also sprouts, which is visible from increasing EVI values in autumn and winter of 2013 and 2014. Additionally, after the seasonal maximum, there is no continuous decrease as in all other seasons, but a plateau or saddle point with a small secondary maximum. This shape of the EVI curve indicates a cultivation of

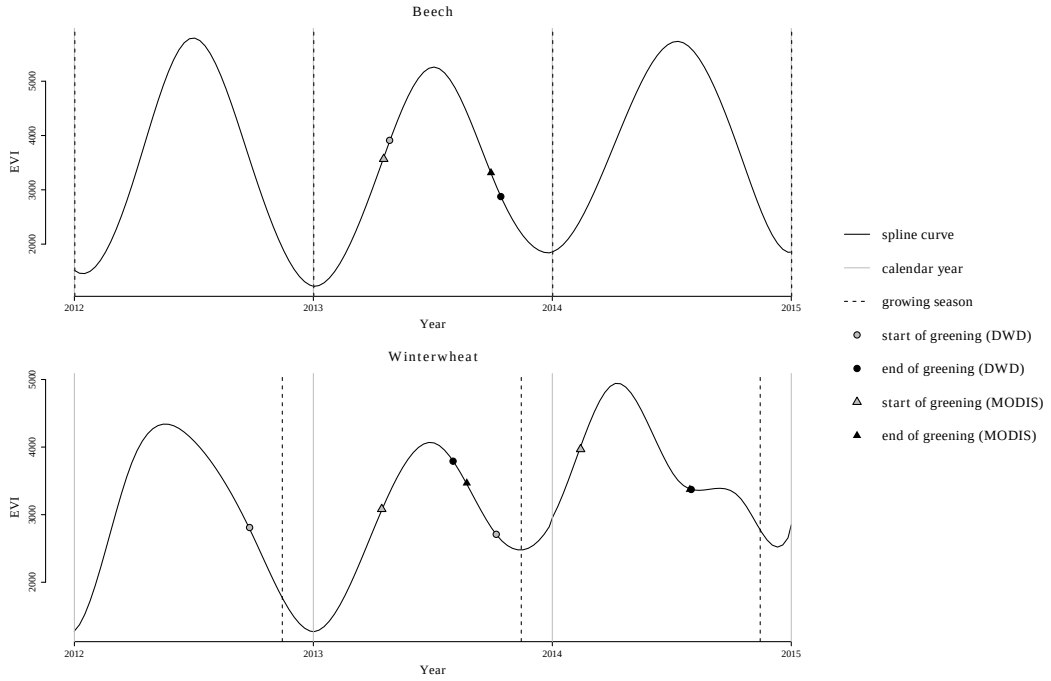

Figure 5.1: Comparison of the growing cycles of Beech (top) and Winterwheat (bottom).

winter crops until harvest in summer, followed by some other crops or vegetated fallow, which causes the secondary maximum. It also leads to a significant shift of the growing cycle against the calendar year. Hence, the reference data place the SOG date for the growing cycle of 2014 in late 2013, while the *phencal* algorithm extracts this date based on the season grid (dashed black lines) and the local extrema, placing it in early 2014.

Coming back to the comparing scatterplot of Winterwheat (see Figure 6.12), the results look worse than they are. The EOG dates are close or around the one-one-line, as for the other species, but the green point clouds for the SOG actually represent a mixture of two years. The x-values, given by the DWD reference, belong to the next respective year, while the y-values are provided by *phencal*, which has problems dealing with growing cycles as shown in Figure 5.1. The effect is even intensified by the window sampling method, which was used to produce the scatterplots, because it causes a mixing of pixels which may differ significantly in land cover and therefore, in their respective values for the phenological descriptors.

For just a few DWD stations, *phencal* was able to detect the actual SOG, as indicated by some green dots near the one-one-line in 2001, 2007 or 2014 (see Figure 6.12), which is very promising. Maybe a more detailed spline model with more knots, representing the original time series more accurately, or a smaller sampling window would increase the performance in such difficult, highly dynamic cropping areas.

With total differences of $6.5, 7, 9$ and 12.5 days (for the respective "optimal" g), compared to the DWD reference data, the prediction uncertainty for the modelled SOG is in a similar category as the methods described by SOUDANI ET AL., HMIMINA ET AL. and BÖTTCHER ET AL.. But their reference data came from own observations on small-scale, homogeneous stands, in contrast to the uncertain phenological observations provided by the DWD. If this uncertainty is taken into account, with the orthogonal difference to the one-one-line as a measurement for the "goodness of fit", the time lag of the prediction decreases by almost three days. Additionally, the studies described in Section 1.2 mostly dealt with specific land use types or plant species instead of the very general, overall approach presented here. KÜBERT deals with the same reference data and therefore the same problems, but has not yet published any results from the evaluation of the *TIMESAT*-derived phenological parameters.

Though using remote sensing data with a resolution that is thought to be too coarse for such an inhomogeneous study area like Germany, with reference data that is highly error-prone in a very general, global modelling approach, the results are overall very promising. The values for the phenological descriptors are reasonable, which matches the first hypothesis of this study. Winter crops cause problems due to their shifted growing cycle, especially when they are associated with intermediate crops or fallow within one year. Some of the descriptors represent the main land use patterns, as stated in the second hypothesis, others do not. But with a combination of different parameters, it should be possible to get a similar classification result as given by the CLC data. The third hypothesis implied consistency within land use classes, which, for the most part, could

not be approved. The inner-annual variabilities of SOG and EOG differ strongly, from nearly zero up to roughly 30 days, while the inter-annual differences are class-dependent, but as well show fluctuations up to a month. Hence, the findings of Bradley et al. (2007) for prairie vegetation from the United States (see Section 1.2) can be transferred to Germany for the most part, and the initial hypothesis of consistent phenological parameters within land use types has to be neglected. But it has to be stressed, that not only the modelling approach has been very general, but also the assignment of the plant species to the respective land use classes. Therefore, it is possible that more detailed reference data would lead to a more exact differentiation of land use classes and plant species and thus, would result in more consistent phenological parameters within these classes.

5.2 Data quality

The results of every scientific analysis strongly rely on the input data, because it is the foundation of the whole study. Bad quality data will therefore mostly result in unreasonable outcomes. This study dealt with completely disparate kinds of input data with different purposes, scientific documentations and quality. The MODIS EVI data, which have been used for the time series, are very well documented and result from automatic processing of the raw reflectance data collected by the satellite system. Advances in hard- and software as well as improvements in the algorithms, which create the final scientific products, have led to very well known and proven datasets. In case of this study, the VI products of *Collection 5* have their own user's guide, are very well documented and come with a set of quality flags, indicating the reliability of every single pixel (Solano et al., 2010). These flags are used within the *splits* framework to perform a weighted fit: the worse the quality of the input pixel, the lower the weight within the fit will be, which should increase the quality of the model. As stated by Huete et al. (2002), Colditz et al. (2009) or Cunha et al. (2010), the overall quality, accuracy and sensitivity of MODIS VI products is very good. Errors or unreliable values

in the outcomes of this study most probably do not result from deficient MODIS input data. Since they are 16-day composites, using the 8-day or even the daily VI products would make it possible to model the actual development of vegetated surfaces more accurately. But the more detailed and therefore bigger datasets lead to much higher computation times, and the effect is thought to be marginal, because the raw data have to be modelled anyway. The accompanied smoothing effect would very likely neutralize the gain from a more detailed raw time series.

In contrary to the MODIS products, the phenological reference data from the DWD are collected by volunteers, following only rudimentary guidelines and recommendations with only little supervision (as described in Section 2.2). The data are also flagged with quality indices, but overall, the user relies completely on the diligence and experience of the volunteer. Additionally, though the locations for the phenological stations are apparently fixed, choosing the observation radius is also up to the volunteer, who is only recommended to use a radius of $\sim 2\ km$. Nonetheless, the biggest issue is the uncertainty in regards of the actual land cover at each phenological station. The occurrence of a plant species is seemingly connected to a geographic location, but in fact, it only can be found somewhere within the observation radius around that station. By this it might happen, that plants are associated with a location where they actually do not occur. In combination with the very heterogeneous study area, where different land use and particularly land cover classes change rapidly over small distances, this poses a very big problem when it comes to evaluating spaceborn VI data. It is not only possible that an observed plant species does not even occur in a specific pixel associated with that coordinate, but it is also very unlikely that the pixel region is completely covered by only one species. This scale-related problem has been targeted with the CLC dataset, which is very well documented, widely used and has a high accuracy (Trombik and Hlásny, 2013). Of course, this still did not provide the actual land cover or reflect the true complexity of german land cover patterns, but at least, it is a good estimation and helped to divide the huge amount of phenological stations into the main land use classes and the most important plant species

within them.

5.3 Processing

The scope for this study has been set up from the beginning, with the *splits* framework and the recently published DWD data right at hand. Though the outcomes are very promising, it is uncertain how the applied methods perform in comparison to other approaches. Results from KÜBERT are yet to be published, and other studies with the same (or similar) data, but different methods have not yet been carried out. Thus, it is difficult to evaluate the processing chain in comparison to other techniques. Furthermore, this study should mark a new application for the recently developed *splits*, which excluded other methods from the start.

In the *splits* framework, splines with different attributes can be set up. But in contrary to the modelling approach by BRADLEY ET AL. (2007), the model neither needs an iterative approach nor high orders or average fits for baselines and envelopes for stabilization. The splines are purely data-driven and can be applied very easily, while being efficient in computation time. Although they have proven to be as good as any other modelling method (MADER, 2012), there may be some room for improvements in setting up an appropriate spline. Since the phenological descriptors are then derived from that spline, the outcome, and by association the evaluation, directly depend on the goodness of that mathematical representation of the original time series. The *splits* framework does not include a validation tool for the fitted model, but uses a least squares method to fit the chosen spline to the data (MADER, 2012). As for now, the user chooses it by visually comparing splines with different attributes, which results in very good approximations for certain pixels, but potentially bad ones for others. This issue might be overcome by setting up different models and evaluating them for the whole image. By giving a threshold of the minimum explained variance, the one spline with the least knots, but still enough level of detail could be chosen. Of

course, this threshold itself would be subjective to some extent and the procedure presumably very (computation) time consuming, but at least it would result in an intermediate spline model, which is more or less suitable for each land cover class. A single model for each pixel would also be conceivable, again with a threshold of the variance the spline would have to explain. The according algorithm would then analyse the time series for every pixel, iteratively test different spline models until it reaches the threshold and then use this model for the actual extraction of the phenological parameters. This approach would take even more time for processing, but would lead to a well fitted model for each pixel. Of course, this is beyond the recent capabilities of *splits*, but may serve as a suggestion or long-term objective for future approaches.

Nonetheless, the processing chain besides the EVI time series has evolved purely from the issues of dealing with modest, uncertain data in a very complex evaluation process. Organizing the raw DWD data in an appropriate, usable way has been more difficult than expected. Presumably, setting up a database and handling the data via *SQL* might have been faster and more easy to repeat. Since no data on the actual dominant plant species at each phenological station were available, the CLC classification has been used to subset them by the main land use class. Representative species of these classes have then been selected to serve for the evaluation of the modelled phenological parameters. Without exact knowledge of the real conditions at each DWD station, this method is obviously very ambitious, but without any alternative. To overcome the problem of the huge differences in spatial scale between the reference and the remotely sensed data, window sampling was used to match the spatial resolution of the raster data with the observation radius of the DWD's volunteers. Alternatively, the comparison between the MODIS-derived and the reference phenological descriptors might have been achieved by point sampling, neglecting the fact that the observation radius for the phenological station is (within a certain range) up to the volunteer's choice.

For single years, the above mentioned *LUCAS* data can be used to overcome this problem. They provide information about the actual land cover, which might

be assigned to the closest respective DWD station, assuming no change within that distance. Or vice versa, using the DWD stations to assign the phenological dates to the respective dominant species at the closest *LUCAS* point. This would give the actual land cover under the assumption, that the entry dates for the phenological phases do not change over that distance. As mentioned in Section 2.3, plant phenology is strongly influenced by small-scale environmental variables (Bijalwan et al., 2013, Dahlgren et al., 2007, Jackson, 1966), but this supposition might be more realistic than the one of consistent land cover. Though not the whole time series can be evaluated with this approach, it probably would be the best for single years.

The scatterplots, illustrating the match between the modelled and the reference phenological dates, work well for plants with a growing cycle that matches the calendar year. But for those whose season is shifted or of another length, they are very confusing, as shown for Winterwheat in Section 5.1. Hence, they might be revised to show not just a single year, but a timeline with the most suitable growing season for each species from the reference data. By this, such plots for winter crops would span two years, making it possible to compare the phenological dates more accurately.

Future studies might not only use other, maybe more advanced methods and new data coming up, but also might have a closer look at specific regions for further investigations. It would be especially interesting to find the reason for the huge misclassification of agriculture in the northwest, as well as for other parts of Germany. Additionally, a suitable classification approach, taking all phenological parameters into account, can be set up and be compared to the CLC data, using not only visual inspection, but statistical descriptors. By this, it might be possible to not only divide the land surface into different land use, but also land cover classes, for which the clear visibility of vineyards in some of the maps described above is very promising.

6

Conclusions

In this thesis, phenological descriptors for Germany have been extracted from a remotely sensed VI time series using a spline-modelling approach. The results have been compared to ground based observations from the DWD, revealing a strong dependency not only on the land cover, but also the greenness parameter g, which is necessary to determine the onset of greening during the growing season. It has become clear, that this value is species-dependent and remains crucial for the estimation of suitable phenological parameters. For forest stands, especially for deciduous trees, the results for SOG and EOG are in good agreement with the reference data, with differences of $\sim$ 5 to 10 days for the former. Winter crops cause problems in deriving the appropriate growing season, because they are often associated with intermediate crops or fallow, which results in distorted VI signals for that respective growing cycle.

The spatial distribution of the phenological parameters can represent land use classes, which may be used in future classification frameworks to distinguish not only certain land use, but also land cover types (meaning dominant plant species). Variations of the descriptors within these classes are mostly very high, probably being the result of the very heterogeneous study area and the estimation of the actual plant species at the reference stations. Likewise, the latter has shown to be the biggest issue of this study, which leaves the most room for improvements. The data from the pan-European *LUCAS* surveys can be used for single years, when appropriately combined with the DWD data.

The *splits* framework has proven to be a very handy tool to set up an appropriate spline model for a VI time series as well as to extract phenological parameters

from it. Though splines with different properties have to be evaluated visually concerning their appropriateness or representative quality for the raw data, the tool has proven to be able to achieve overall reasonable results. Compared to other studies, which mostly dealt with small, homogeneous regions and in-situ reference measurements, the outcomes of this very general approach for a large-scale, heterogeneous study area are very promising and might become even better with more detailed reference data.

Bibliography

Bijalwan, R., Vats, M., and Joshi, S. P. (2013). Plant phenological response to microclimatic variations in an alpine zone of Garhwal Himalaya. *Journal of Applied and Natural Science*, 5:47–52.

Böttcher, K., Aurela, M., Kervinen, M., Markkanen, T., Mattila, O.-P., Kolari, P., Metsämäki, S., Aalto, T., Arslan, A. N., and Pulliainen, J. (2014). MODIS time-series-derived indicators for the beginning of the growing season in boreal coniferous forest — A comparison with CO_2 flux measurements and phenological observations in Finland. *Remote Sensing of Environment*, 140:625–638.

Bradley, B. A., Jacob, R. W., Hermance, J. F., and Mustard, J. F. (2007). A curve fitting procedure to derive inter-annual phenologies from time series of noisy satellite NDVI data. *Remote Sensing of Environment*, 106:137–145.

Bundesministerium für Bildung und Forschung (BMBF) (2015). Fruchtfolge. http://www.pflanzenforschung.de/de/themen/lexikon/fruchtfolge-1521/. retrieved: 2014-06-30.

Bundesministerium für Ernährung und Landwirtschaft (BMEL) (2014a). Betriebe mit Anbau von Hauptkultur- und Fruchtarten nach Größenklassen der landwirtschaftlich genutzten Fläche 2010. http://berichte.bmelv-statistik.de/SJT-3070700-2010.pdf. retrieved: 2014-10-14.

Bundesministerium für Ernährung und Landwirtschaft (BMEL) (2014b). Der Wald in Deutschland - Ausgewählte Ergebnisse der dritten Bundeswaldinventur. https://bundeswaldinventur.de/fileadmin/SITE_MASTER/content/Dokumente/Downloads/BMEL_Wald_Broschuere.pdf. retrieved: 2015-04-30.

Colditz, R. R., Conrad, C., Wehrmann, T., Schmidt, M., and Dech, S. (2009).

Analysis of the Quality of Collection 4 and 5 Vegetation Index Time Series from MODIS, chapter 13, pages 161–174. CRC Press - Taylor & Francis Group, London, United Kingdom.

Cong, N., Piao, S., Chen, A., Wang, X., Lin, X., Chen, S., Han, S., Zhou, G., and Zhang, X. (2012). Spring vegetation green-up date in China inferred from SPOT NDVI data: A multiple model analysis. *Agricultural and Forest Meteorology*, 165:104–113.

Cunha, M., Poças, I., Marcal, A. R., Rodrigues, A., and Pereira, L. S. (2010). Evaluating MODIS vegetation indices using ground based measurements in mountain semi-natural meadows of Northeast Portugal. In *IEEE International Geoscience & Remote Sensing Symposium, IGARSS 2010, July 25-30, 2010, Honolulu, Hawaii, USA, Proceedings*, pages 1525–1528.

Dahlgren, J. P., von Zeipel, H., and Ehrlén, J. (2007). Variation in vegetative and flowering phenology in a forest herb caused by environmental heterogeneity. *American Journal of Botany*, 94:1570–1576.

de Boor, C. (1972). On calculating with B-splines. *Journal of Approximation Theory*, 6:50–62.

Deutscher Wetterdienst (DWD) (2012). Phänologische Beobachtungen - wesentliche Punkte der Beobachtungsrichtlinien. http://www.dwd.de/bvbw/appmanager/bvbw/dwdwwwDesktop?_nfpb=true&_pageLabel=dwdwww_result_page&portletMasterPortlet_i1gsbDocumentPath=Navigation%2FOeffentlichkeit%2FKlima__Umwelt%2FPhaenologie%2Fallgemeines%2Fkurzfassung__node.html%3F__nnn%3Dtrue. retrieved: 2015-01-05.

Deutsches Statistisches Bundesamt (DESTATIS) (2013). Flächennutzung - Bodenfläche nach Nutzungsarten. https://www.destatis.de/DE/ZahlenFakten/Wirtschaftsbereiche/LandForstwirtschaftFischerei/Flaechennutzung/Tabellen/Bodenflaeche.html. retrieved: 2015-06-28.

Didan, K. and Huete, A. (2006). MODIS Vegetation Index Product Series Collection 5 Change Summary. http://landweb.nascom.nasa.gov/QA_WWW/forPage/MOD13_VI_C5_Changes_Document_06_28_06.pdf. retrieved: 2015-01-05.

Eklundh, L. and Jönsson, P. (2015). TIMESAT 3.2 with parallel processing - Software Manual. http://web.nateko.lu.se/timesat/docs/TIMESAT32_software_manual.pdf. retrieved: 2015-05-26.

ESRI Resource Center, ArcGIS Help 10.1 (ESRI Help) (2012). Extract values to points (spatial analyst). http://resources.arcgis.com/en/help/main/10.1/index.html#/Extract_Values_to_Points/009z0000002t000000/. retrieved: 2015-05-26.

European Environment Agency (EEA) (2007). Corine Land Cover 2006 raster data. http://www.eea.europa.eu/publications/technical_report_2007_17. retrieved: 2014-10-09.

European Environment Agency (EEA) (2013). Corine Land Cover 2006 raster data. http://www.eea.europa.eu/data-and-maps/data/corine-land-cover-2006-raster-3. retrieved: 2014-10-09.

Faraway, J. J. (2006). *Extending the Linear Model with R*. Texts in Statistical Science Series. Chapman & Hall/CRC.

Fisher, J. I., Mustard, J. F., and Vadeboncoeur, M. A. (2006). Green leaf phenology at Landsat resolution: Scaling from the field to the satellite. *Remote Sensing of Environment*, 100:265–279.

Hmimina, G., Dufrêne, E., Pontailler, J.-Y., Delpierre, N., Aubinet, M., Caquet, B., de Grandcourt, A., Burban, B., Flechard, C., Granier, A., Gross, P., Heinesch, B., Longdoz, B., Moureaux, C., Ourcival, J.-M., Rambal, S., Saint Andréh, L., and Soudani, K. (2013). Evaluation of the potential of MODIS satellite data to predict vegetation phenology in different biomes: An investigation using ground-based NDVI measurements. *Remote Sensing of Environment*, 132(5):145–158.

Huete, A., Didan, K., Miura, T., Rodriguez, E. P., Gao, X., and Ferreira, L. G. (2002). Overview of the radiometric and biophysical performance of the MODIS vegetation indices. *Remote Sensing of Environment*, 83(1-2):195–213.

Jackson, M. T. (1966). Effects of microclimate on spring flowering phenology. *Ecology*, 47:407–415.

Jackson, R. D. and Huete, A. R. (1991). Interpreting vegetation indices. *Preventive Veterinary Medicine*, 11:185–200.

Kübert, C. (2015). Concepts for the assessment and analysis of land surface phenology unsing remote sensing data. http://www.fernerkundung.geographie.uni-wuerzburg.de/en/fernerkundung_neu/dissertations/current_dissertations/carina_kuebert/. retrieved: 2015-06-22.

Kübert, C., Klein, D., Wegmann, M., Conrad, C., and Dech, S. (2011). Multi-sensor-concepts for the assessment of land surface phenology using remote sensing data. http://www.geographie.uni-wuerzburg.de/fileadmin/04140500/Bilder/Diss-Projekte/Carina/20111025_PhenoALP_Kuebert_final.pdf. retrieved: 2015-06-22.

Mader, S. (2012). *A Framework for the Phenological Analysis of Hypertemporal Remote Sensing Data Based on Polynomial Spline Models*. PhD thesis, University of Trier, Universitätsring 15, 54296 Trier.

McMaster, G. S. and Wilhelm, W. (1997). Growing degree-days: one equation, two interpretations. *Agricultural and Forest Meteorology*, 87:219–300.

Meier, J. and Herring, D. (2000). Measuring Vegetation (NDVI & EVI) - Enhanced Vegetation Index (EVI). http://earthobservatory.nasa.gov/Features/MeasuringVegetation/measuring_vegetation_4.php. retrieved: 2015-05-21.

NASA Land Processes Distributed Active Archive Center (LP DAAC) (2014a). Vegetation Indices 16-Day L3 Global 250m, MOD13Q1. https://lpdaac.usgs.gov/products/modis_products_table/mod13q1. retrieved: 2015-01-05.

NASA Land Processes Distributed Active Archive Center (LP DAAC) (2014b). Vegetation Indices 16-Day L3 Global 250m, MYD13Q1. https://lpdaac.usgs.gov/products/modis_products_table/myd13q1. retrieved: 2015-01-05.

National Aeronautics and Space Administration (NASA) (2015a). About. http://modis.gsfc.nasa.gov/about/. retrieved: 2015-08-12.

National Aeronautics and Space Administration (NASA) (2015b). Specifications. http://modis.gsfc.nasa.gov/about/specifications.php. retrieved: 2015-08-12.

Pan, Z., Huang, J., Zhou, Q., Wang, L., Cheng, Y., Zhang, H., Blackburn, G. A., Yan, J., and Liu, J. (2015). Mapping crop phenology using NDVI time-series derived from HJ-1A/B data. *International Journal of Applied Earth Observation and Geoinformation*, 34:188–197.

Prautzsch, H., Boehm, W., and Paluszny, M. (2002). *Bézier- and B-spline techniques*. Springer.

Rubin, J. (1967). Optimal classification into groups: An approach for solving the taxonomy problem. *Journal of Theoretical Biology*, 15:103–144.

Solano, R., Didan, K., Jacobson, A., and Huete, A. (2010). MODIS Vegetation Index User's Guide (MOD13 Series).

Soudani, K., le Maire, G., Dufrêne, E., François, C., Delpierre, N., Ulrich, E., and Cecchini, S. (2008). Evaluation of the onset of green-up in temperate deciduous broadleaf forests derived from Moderate Resolution Imaging Spectroradiometer (MODIS) data. *Remote Sensing of Environment*, 112(5):2643–2655.

Thünen-Institut, Dritte Bundeswaldinventur - Ergebnisdatenbank, https://bwi.info (BWI-3) (2012). Waldfläche (gemäß Standflächenanteil) [ha] nach Land und Baumartengruppe (rechnerischer Reinbestand). https://bwi.info/inhalt1.3.aspx?Text=1.04%20Baumartengruppe%20%28rechnerischer%20Reinbestand%29&prrolle=public&prInv=BWI2012&prKapitel=1.04. retrieved: 2014-10-09.

Trombik, J. and Hlásny, T. (2013). Free European data on forest distribution: overview and evaluation. *Journal of forest science*, 59(11):447–457.

White, M. A., Thornton, P. E., and Running, S. W. (1997). A continental phenology model for monitoring vegetation responses to interannual climatic variability. *Global Biogeochemical Cycles*, 11:217–234.

Wichmann, V. (2005). Module Zonal Grid Statistics. http://www.saga-gis.org/saga_module_doc/2.1.3/statistics_grid_5.html. retrieved: 2015-08-03.

Xiao, W., Sun, Z., Wang, Q., and Yang, Y. (2013). Evaluating MODIS phenology product for rotating croplands through ground observations. *Journal of Applied Remote Sensing*, 7:1–12.

Zhang, X., Friedl, M. A., Schaaf, C. B., Strahler, A. H., Hodges, J. C., Gao, F., Reed, B. C., and Huete, A. (2001). Global vegetation phenology from AVHRR and MODIS data. *Proceedings of the International Geoscience and Remote Sensing Symposium*.

Zhang, X., Hodges, J. C., Schaaf, C. B., Friedl, M. A., Strahler, A. H., , and Gao, F. (2003). Monitoring vegetation phenology using MODIS. *Remote Sensing of Environment*.

Appendix

As mentioned in Section 4.3, the comparing scatterplots for Beech, Oak, Spruce, Pine, Maize and Winterwheat, which have been derived with a greenness parameter g of 0.2 and 0.8, respectively, are shown here. To make the comparison easier, the images are sorted by species instead of the different g values, with 0.20 to the left and 0.80 to the right.

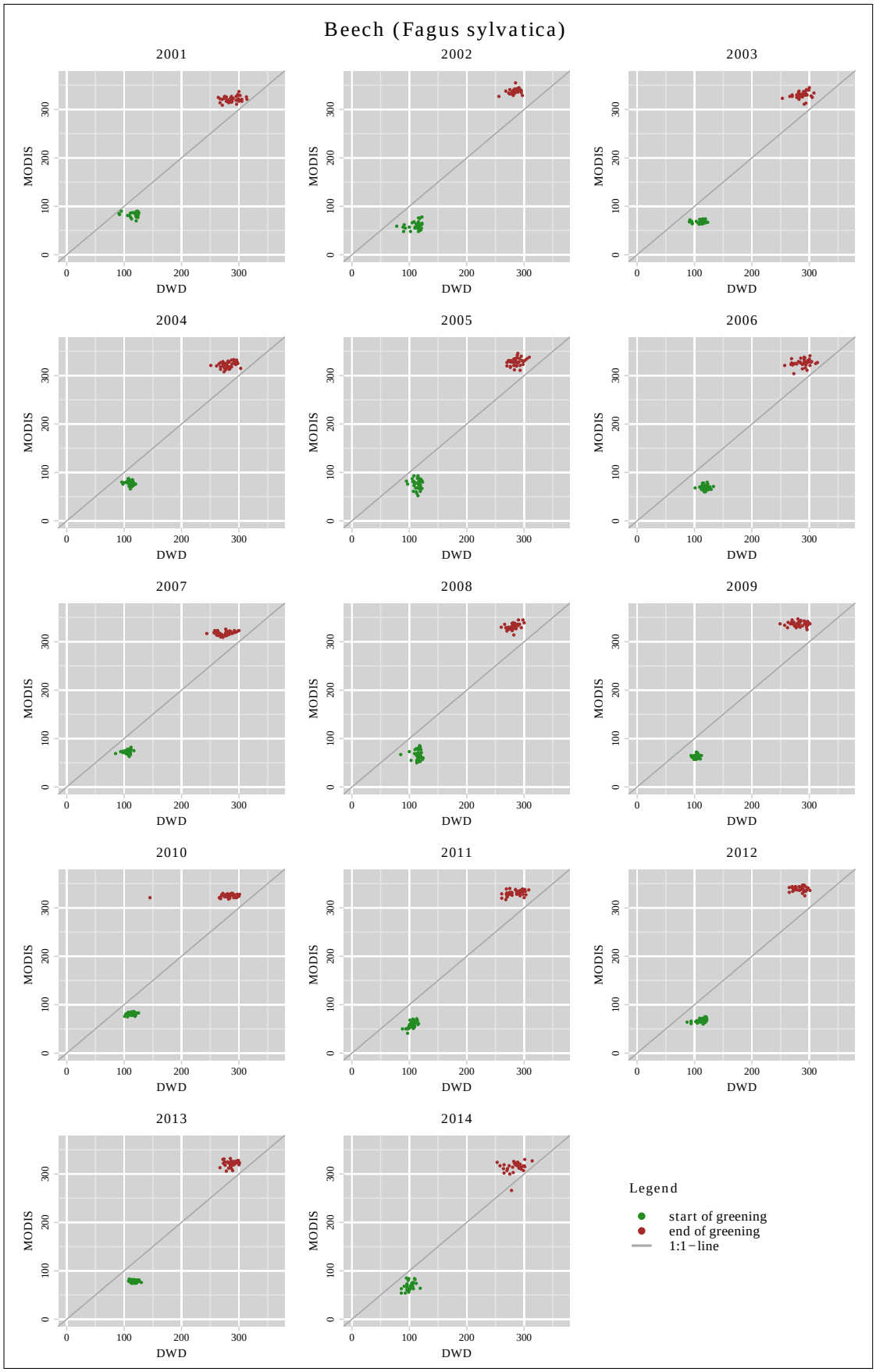

Figure 6.1: DOY comparison for Beech (*Fagus sylvatica*); $g = 0.20$.

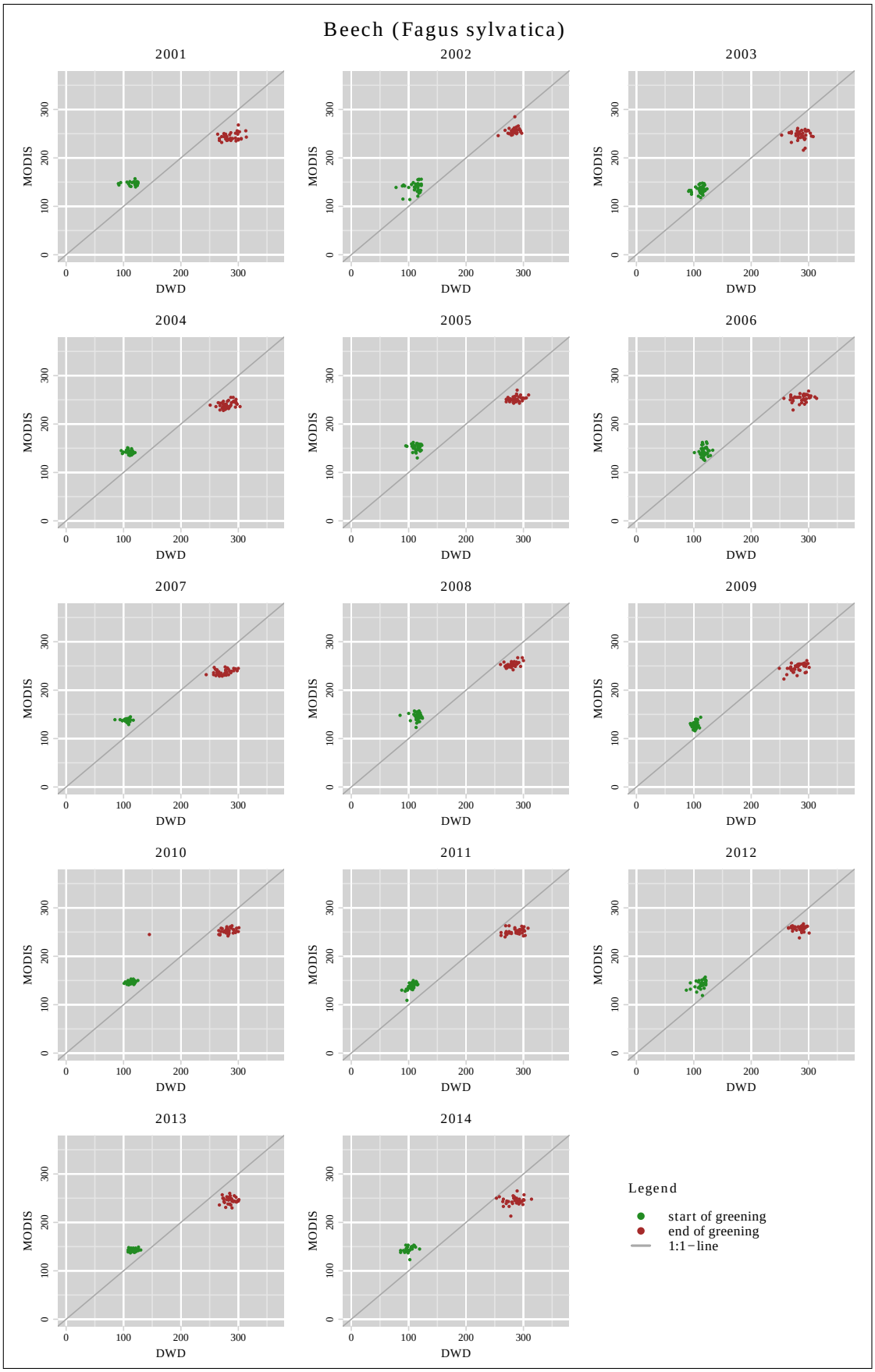

Figure 6.2: DOY comparison for Beech (*Fagus sylvatica*); $g = 0.80$.

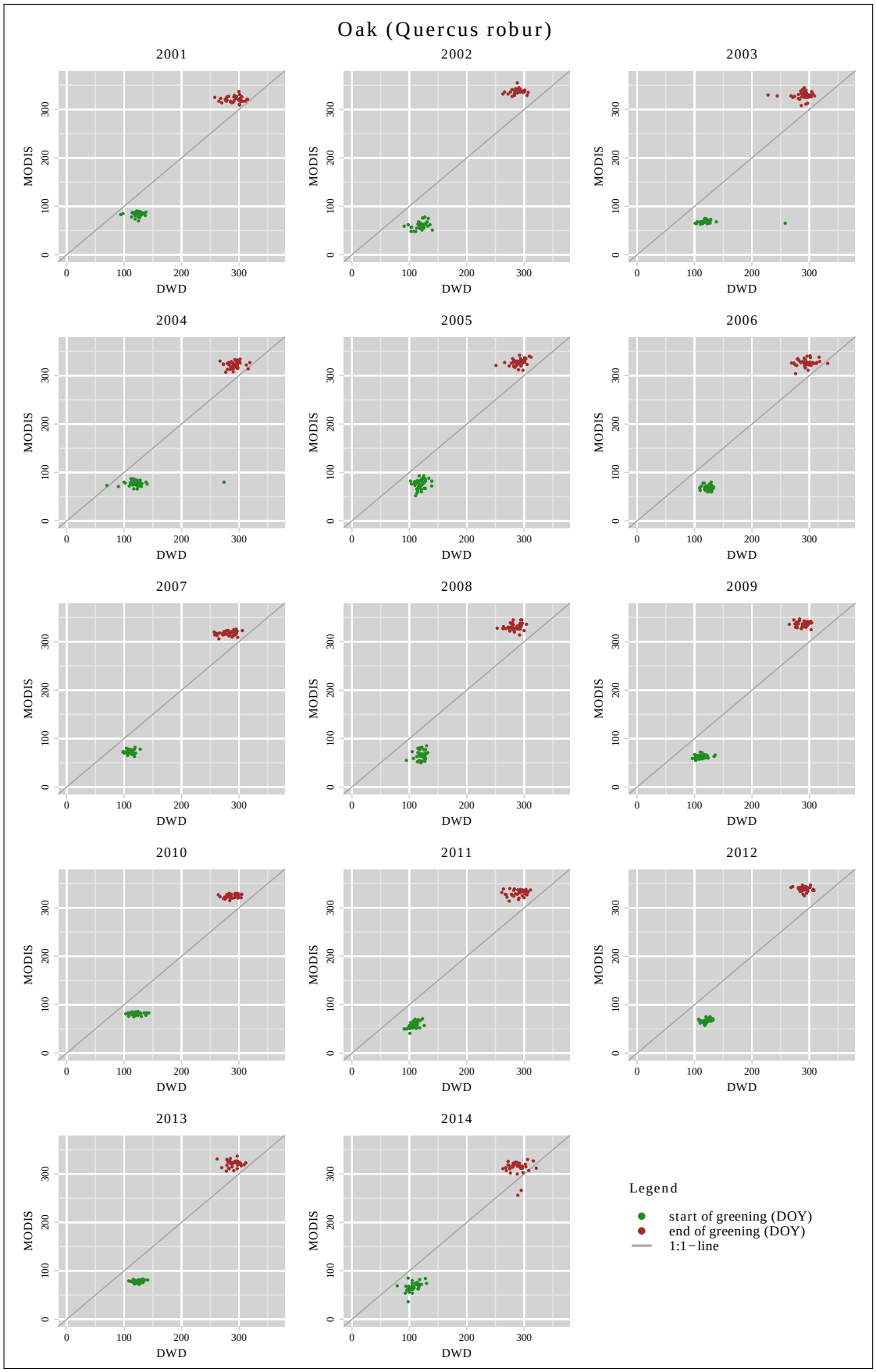

Figure 6.3: DOY comparison for Oak (*Quercus robur*); $g = 0.20$.

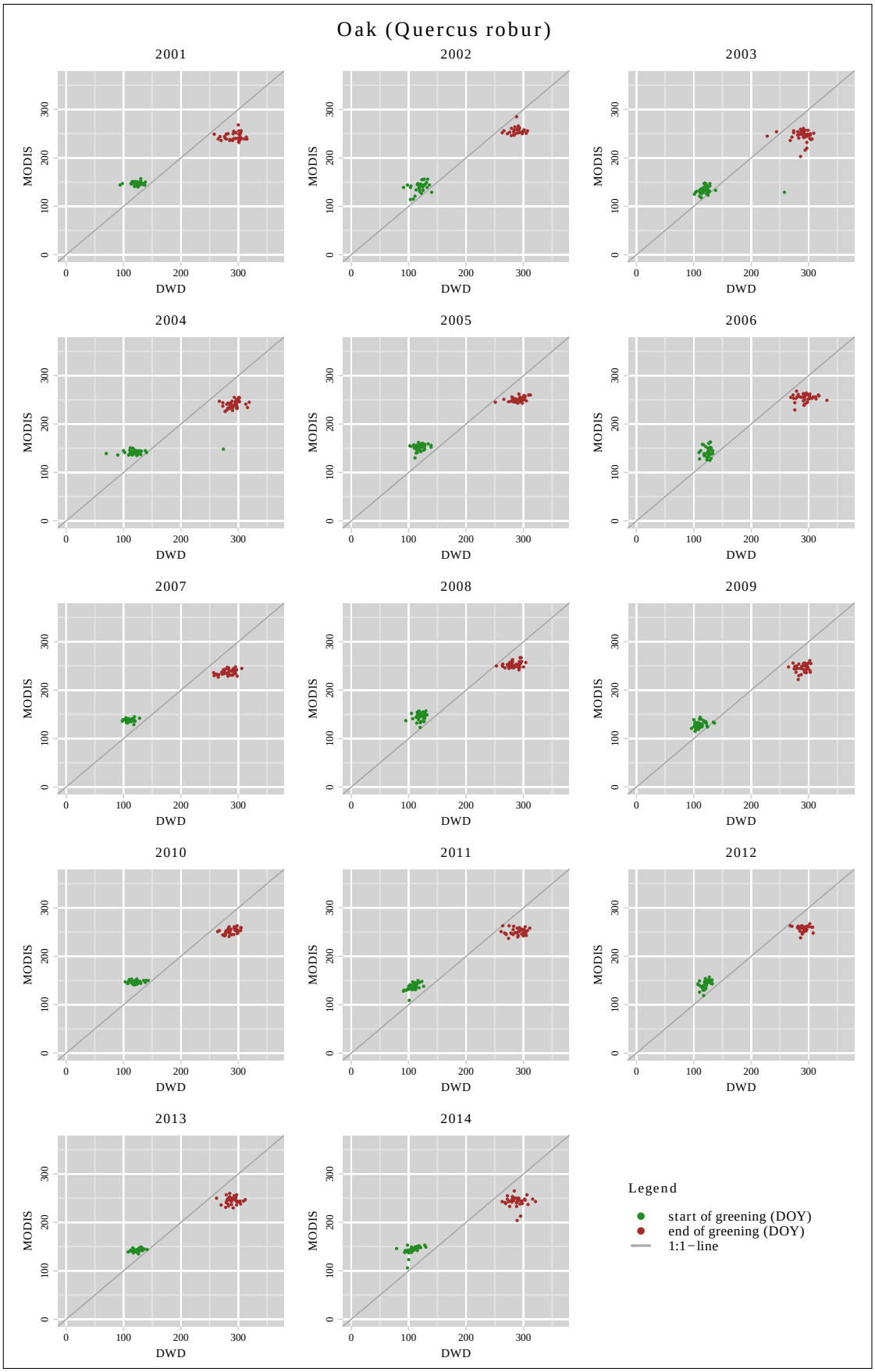

Figure 6.4: DOY comparison for Oak (*Quercus robur*); $g = 0.80$.

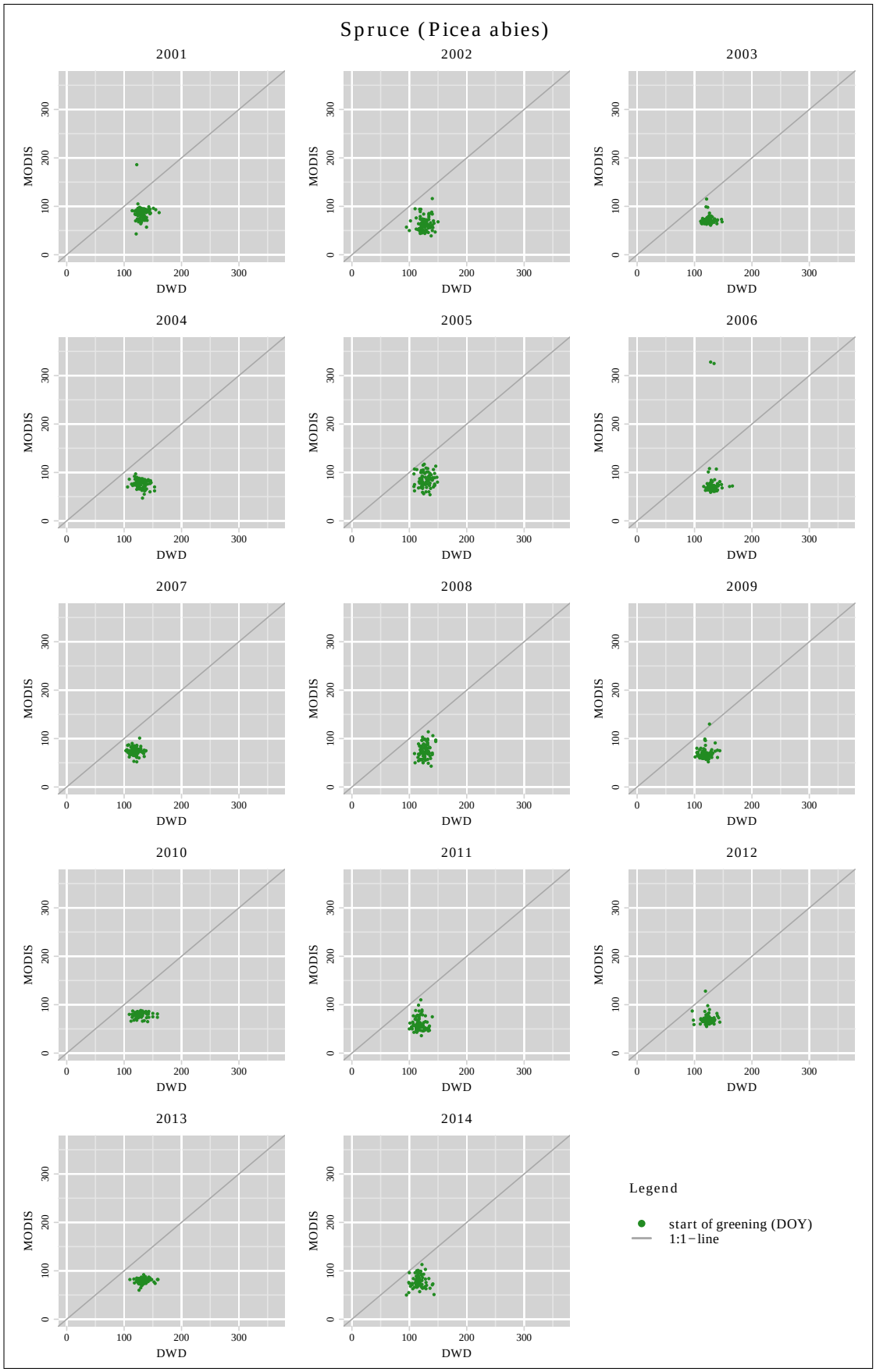

Figure 6.5: DOY comparison for Spruce (*Picea abies*); $g = 0.20$.

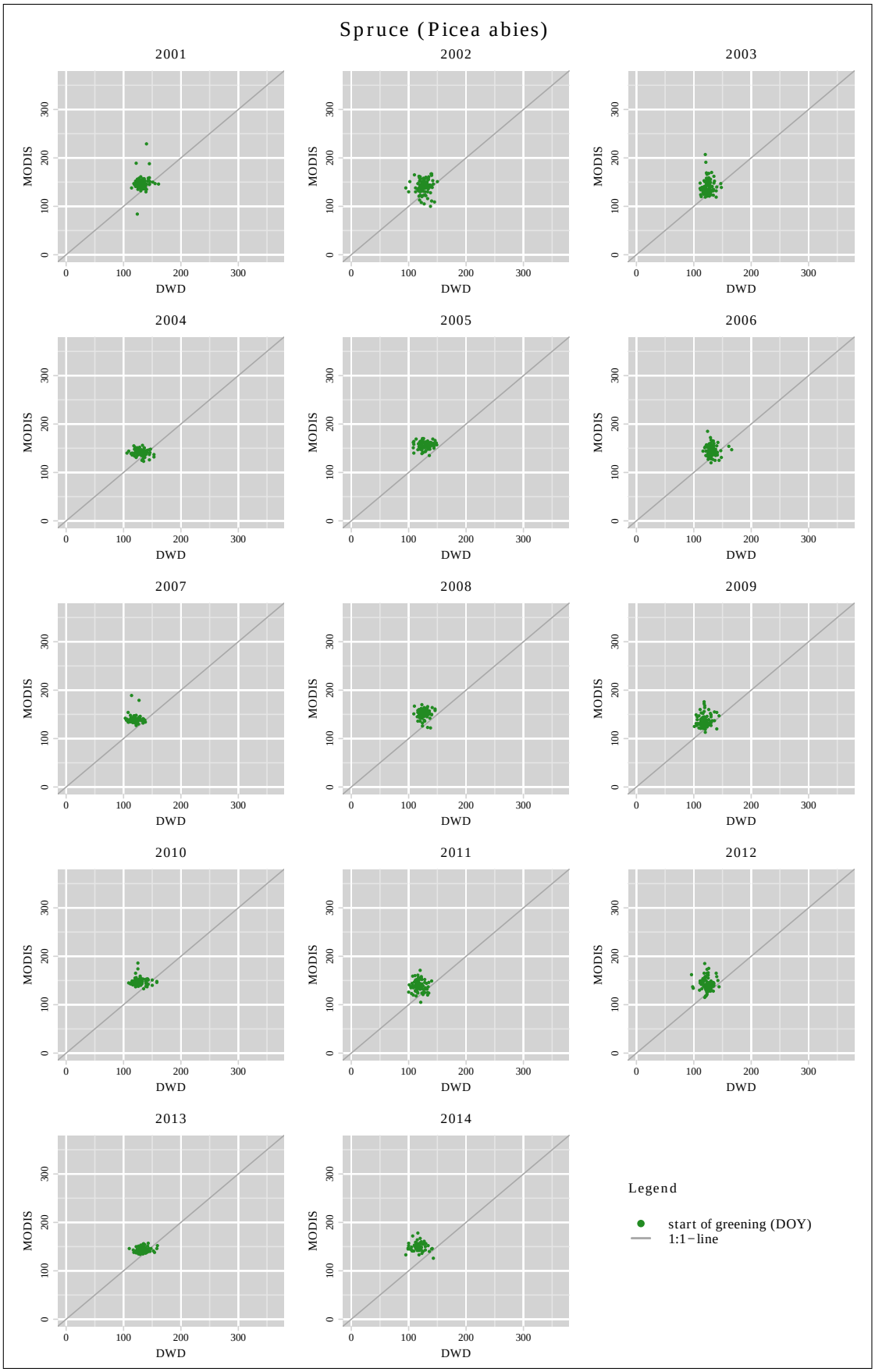

Figure 6.6: DOY comparison for Spruce (*Picea abies*); $g = 0.80$.

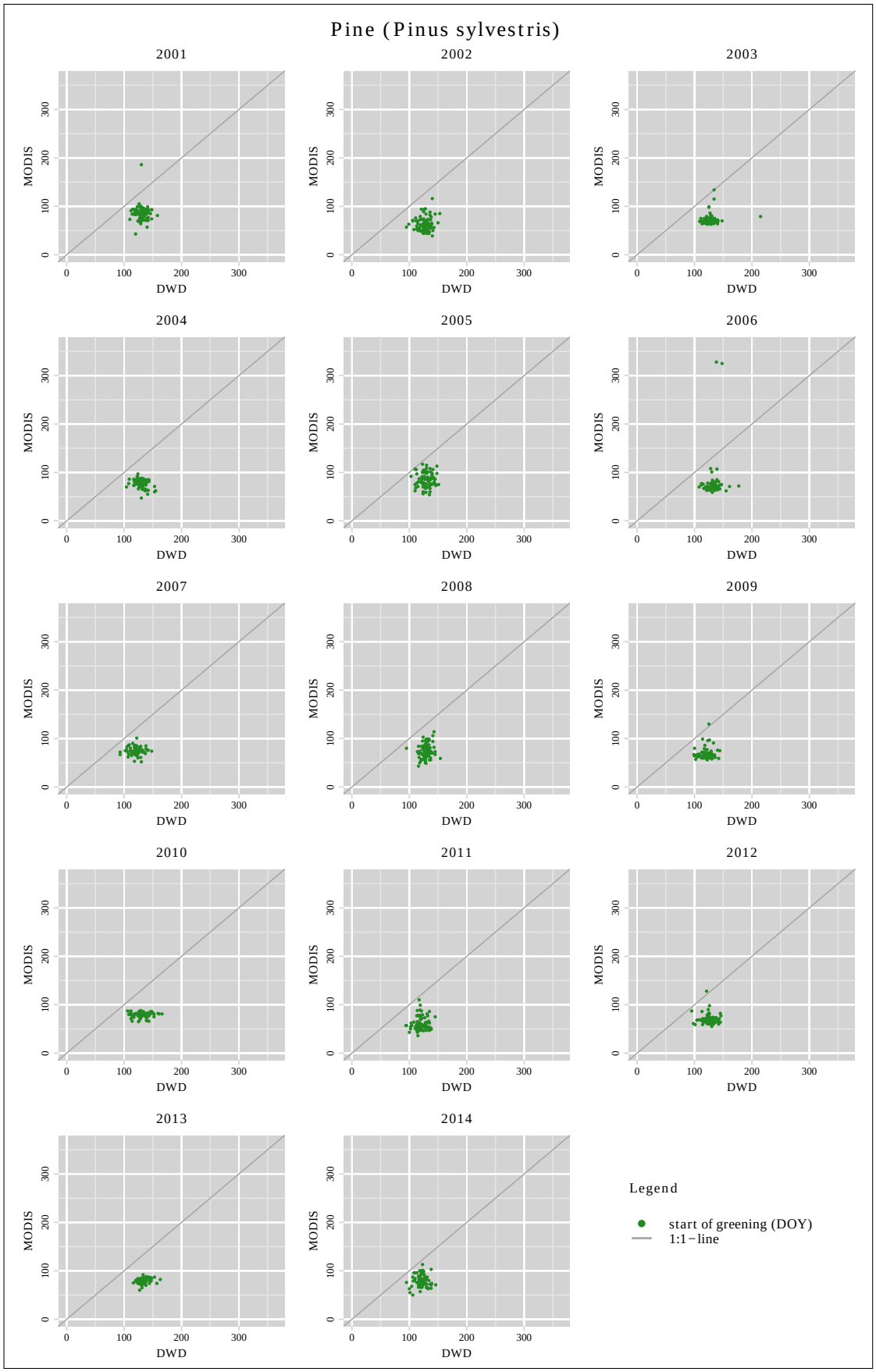

Figure 6.7: DOY comparison for Pine (*Pinus sylvestris*); $g = 0.20$.

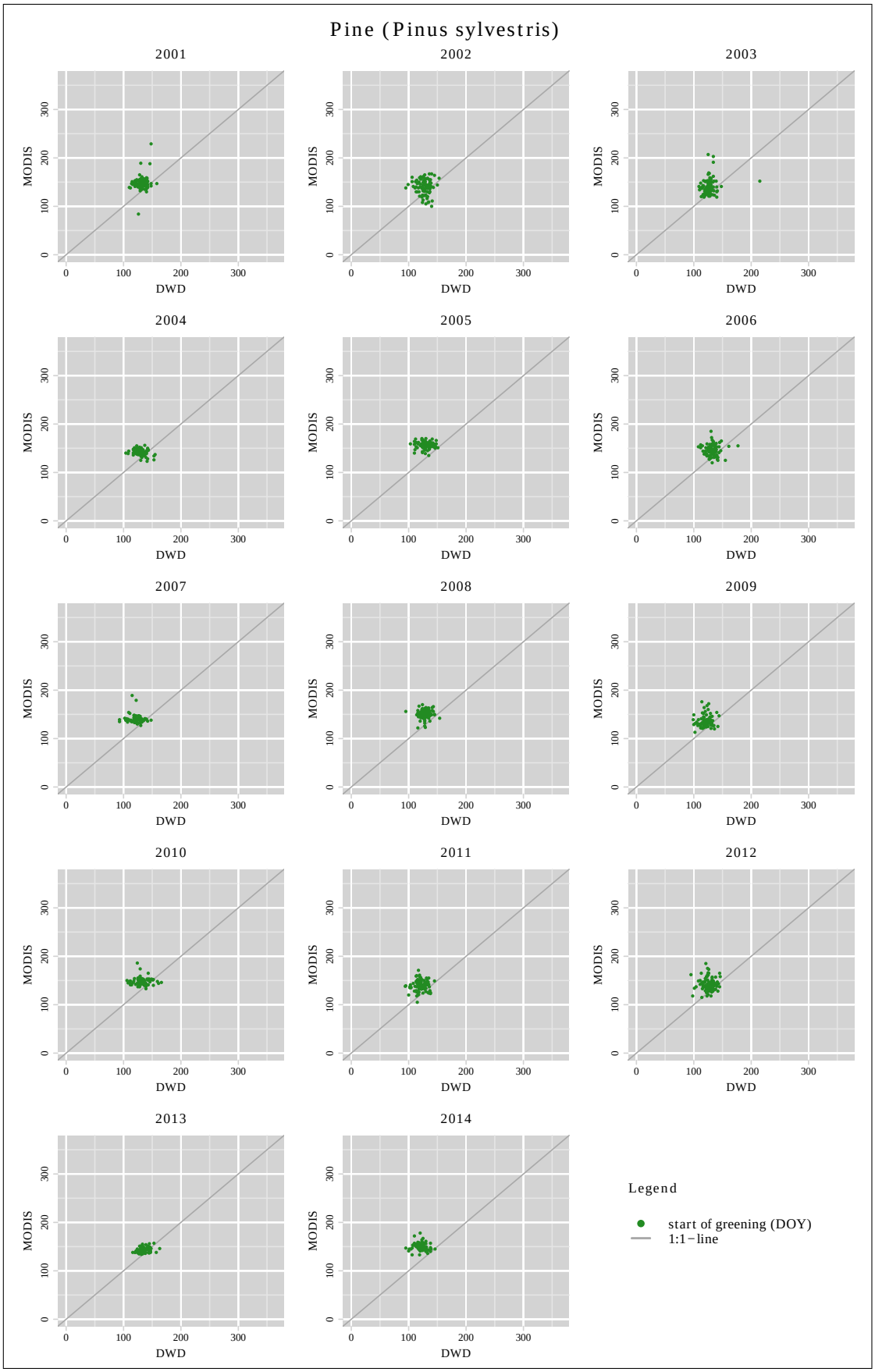

Figure 6.8: DOY comparison for Pine (*Pinus sylvestris*); $g = 0.80$.

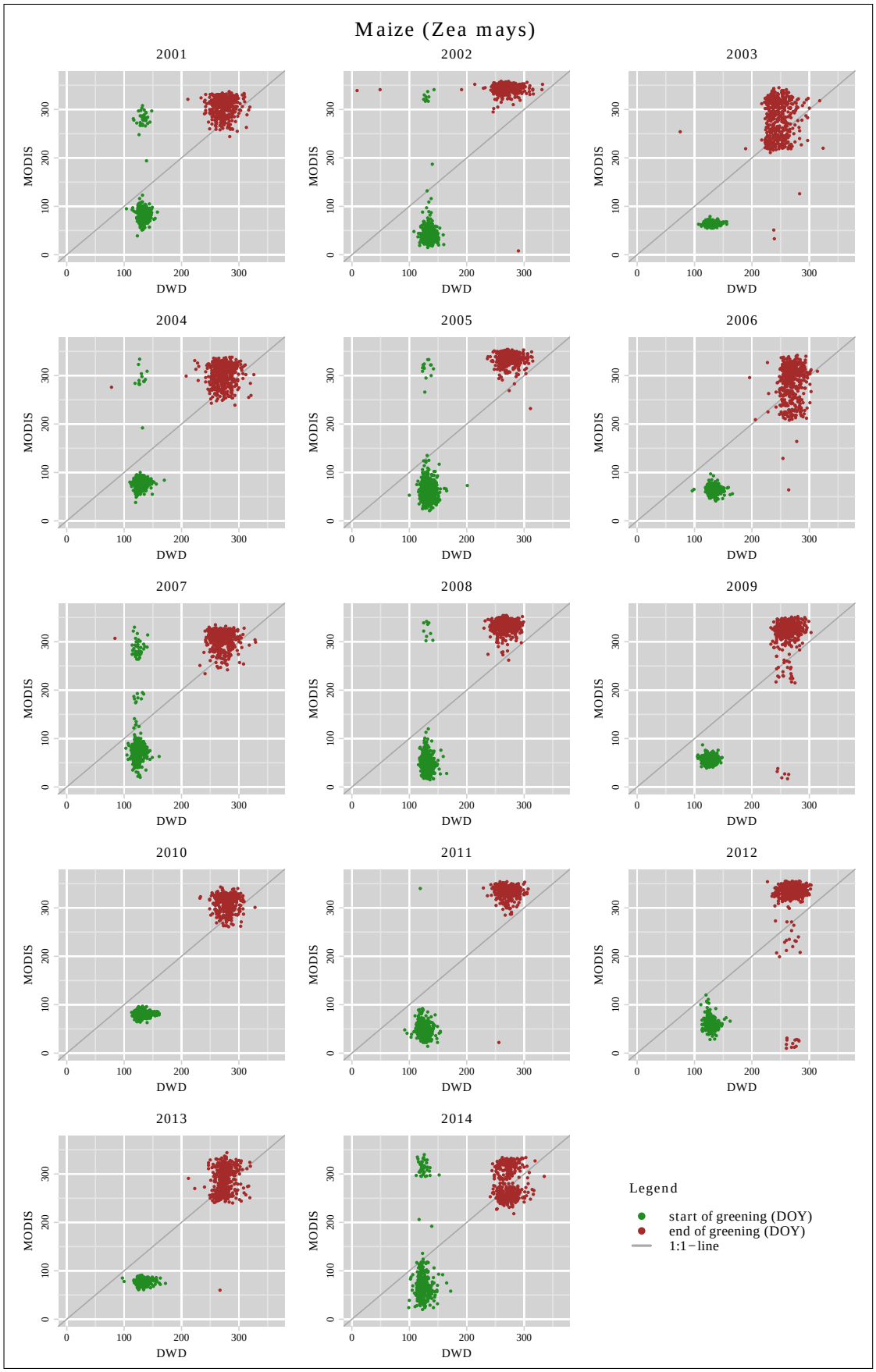

Figure 6.9: DOY comparison for Maize (*Zea mays*); $g = 0.20$.

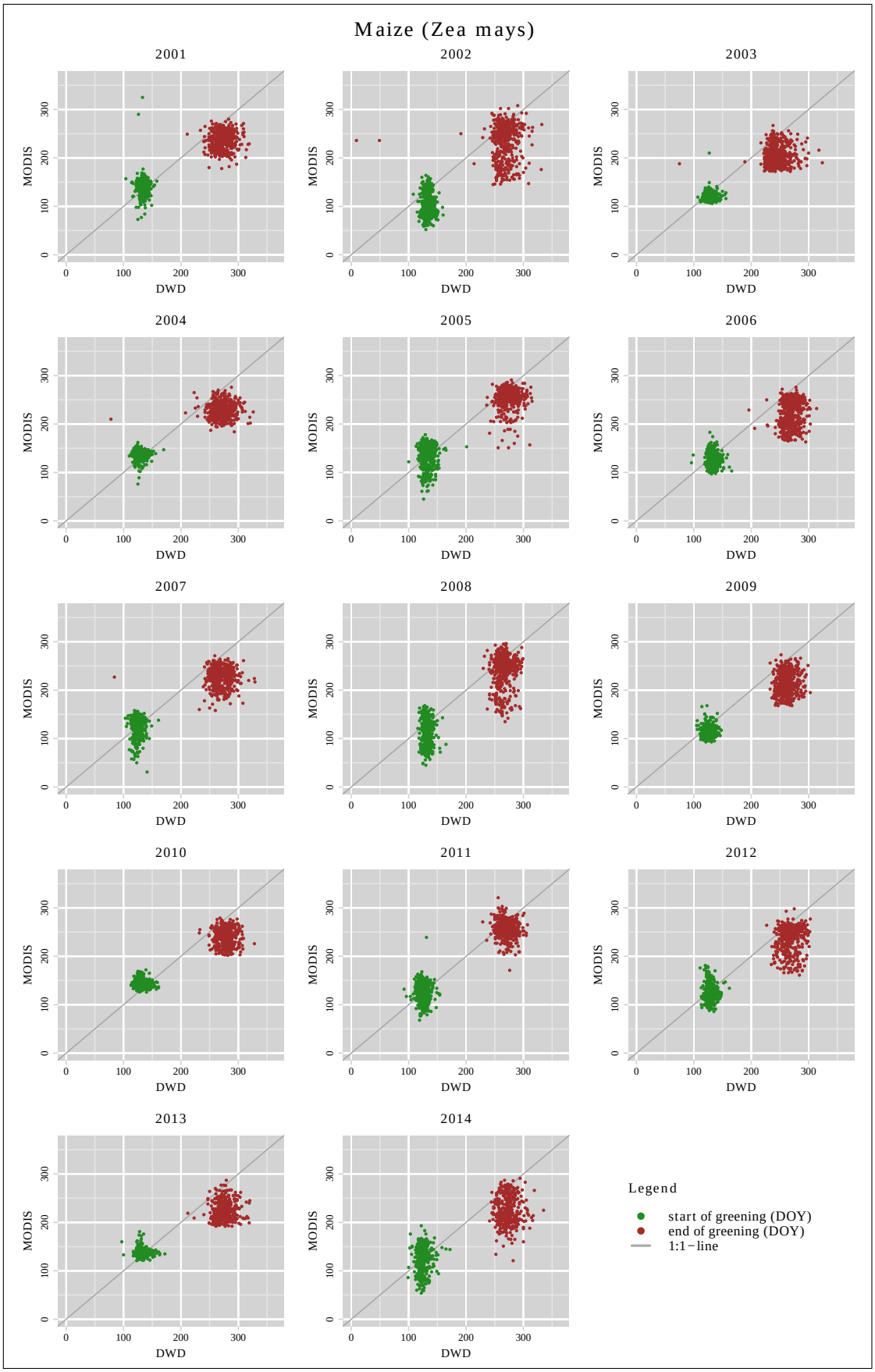

Figure 6.10: DOY comparison for Maize (*Zea mays*); $g = 0.80$.

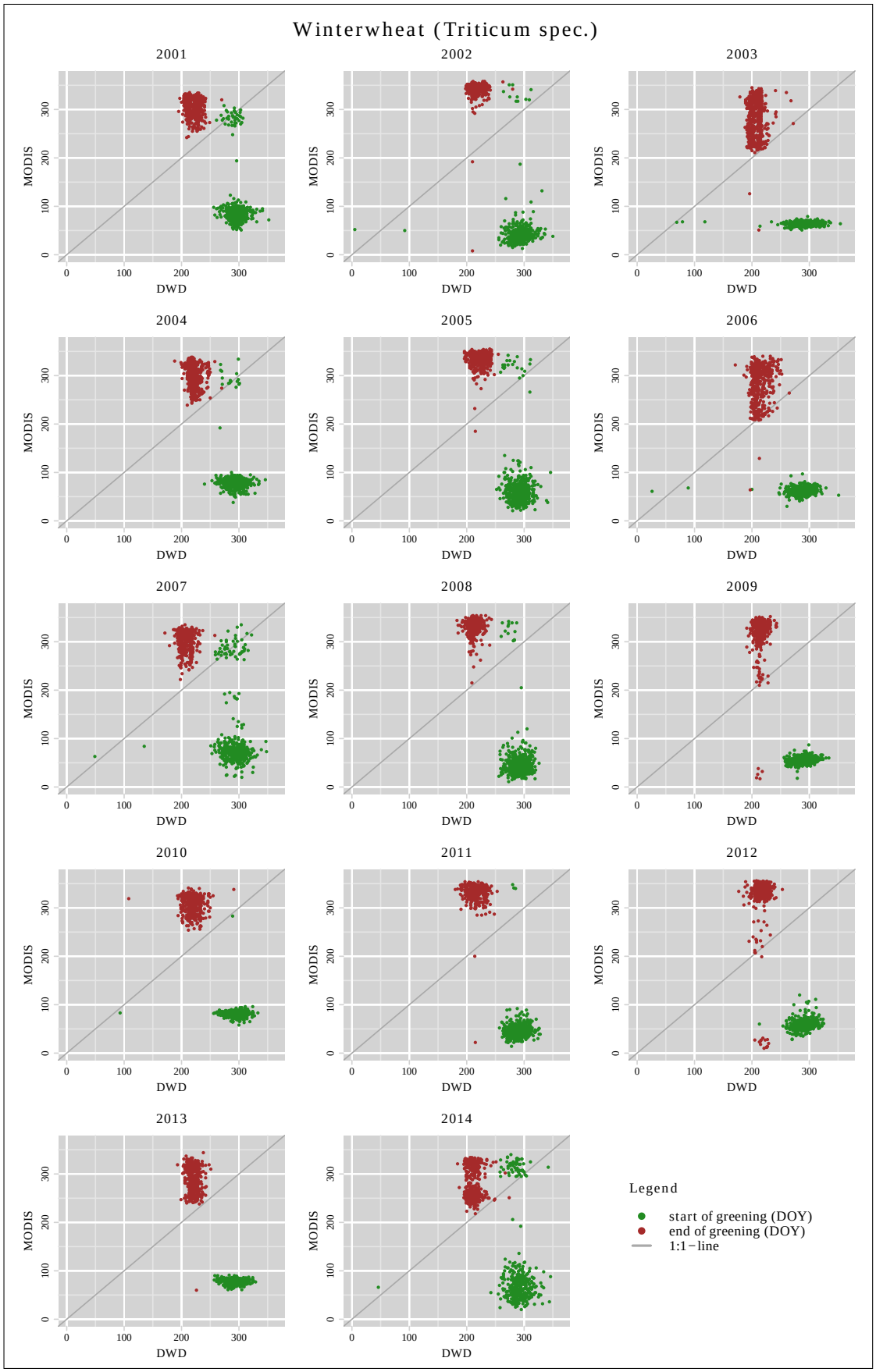

Figure 6.11: DOY comparison for Winterwheat (*Triticum spec.*); $g = 0.20$.

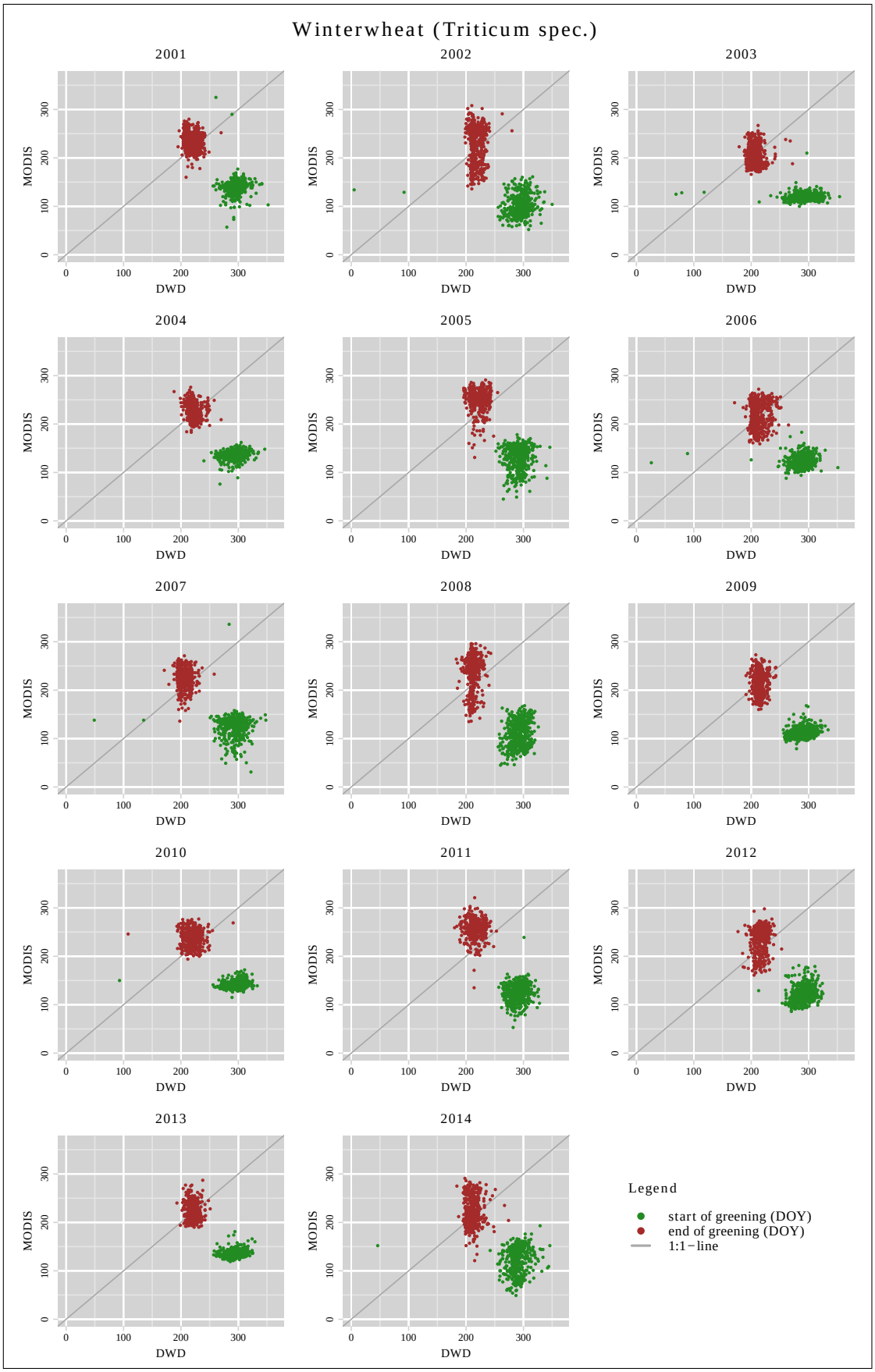

Figure 6.12: DOY comparison for Winterwheat (*Triticum spec.*); $g = 0.80$.

Declaration of authorship

I hereby certify, that this Master thesis has been composed by myself and is based on my own work, unless stated otherwise. No other person's work has been used without due acknowledgement in this thesis. All references and verbatim extracts have been quoted, and all sources of information, including graphs and data sets, have been specifically acknowledged.

Date: September 9, 2015

Signature: